



Acquisition, Maintenance, and Ecological Roles of Kleptoplasts in *Planoglabratella opercularis* (Foraminifera, Rhizaria)

Masashi Tsuchiya^{1*}, Seiji Miyawaki^{1,2}, Kazumasa Oguri¹, Takashi Toyofuku³, Akihiro Tame⁴, Katsuyuki Uematsu⁴, Koji Takeda^{1,5}, Yuya Sakai^{1,5}, Hiroshi Miyake² and Tadashi Maruyama^{1,2}

¹ Research Institute for Global Change (RIGC), Japan Agency for Marine-Earth Science and Technology (JAMSTEC), Yokosuka, Japan, ² School of Marine Biosciences, Kitasato University, Sagami-hara, Japan, ³ Institute for Extra-Cutting-Edge Science and Technology Avant-Garde Research (X-Star), Japan Agency for Marine-Earth Science and Technology (JAMSTEC), Yokosuka, Japan, ⁴ Marine Works Japan, Ltd., Yokosuka, Japan, ⁵ Tokyo College of Biotechnology, Ota-ku, Japan

OPEN ACCESS

Edited by:

Angel Borja,
Technological Center Expert in Marine
and Food Innovation (AZTI), Spain

Reviewed by:

Felisa Rey,
University of Aveiro, Portugal
Thierry Jauffrais,
Institut Français de Recherche pour
l'Exploitation de la Mer (New
Caledonia), New Caledonia

*Correspondence:

Masashi Tsuchiya
tsuchiya@jamstec.go.jp

Specialty section:

This article was submitted to
Marine Ecosystem Ecology,
a section of the journal
Frontiers in Marine Science

Received: 14 May 2020

Accepted: 24 June 2020

Published: 28 July 2020

Citation:

Tsuchiya M, Miyawaki S, Oguri K,
Toyofuku T, Tame A, Uematsu K,
Takeda K, Sakai Y, Miyake H and
Maruyama T (2020) Acquisition,
Maintenance, and Ecological Roles
of Kleptoplasts in *Planoglabratella
opercularis* (Foraminifera, Rhizaria).
Front. Mar. Sci. 7:585.
doi: 10.3389/fmars.2020.00585

Kleptoplasty or acquisition of chloroplasts from ingested photosynthetic organisms, is thought to be a key factor in determining the trophic requirements and carbon mineralization of foraminifera, consequently influencing their ecology, evolution, and calcification. However, the acquisition, maintenance, and functions of “stolen” chloroplasts (kleptoplasts) in foraminiferal cells have not been well characterized. Using molecular phylogeny and experimental measurements of oxygen flux and intracellular (vacuole) pH, we characterized aspects of kleptoplast origin and function in *Planoglabratella opercularis* (d’Orbigny), a rocky-shore benthic foraminifera. We determined that the kleptoplasts in *P. opercularis* are derived from various species of epiphytic diatoms. The acquisition of epiphytic diatoms is congruent with the behavior of *P. opercularis*, which crawls on the thalli of coralline algae and grazes on the microalgae on the algal surface. Kleptoplasts were located near the host foraminiferal cell periphery, just under the pore plug, mainly along the dorsal side, which is important for oxygenic photosynthesis. The lifespan of kleptoplasts varied according to food availability and to the intensity and duration of light irradiation. *Planoglabratella opercularis* was able to capture not only diatom chloroplasts but also those from *Chlorella*. Kleptoplastids of diatom origin decreased in autofluorescence and were digested within 11 days under light in the absence of food. This suggests that host foraminifera frequently capture new diatoms to sustain kleptoplasts. Kleptoplastid autofluorescence was prolonged in the dark or 24:24-h light:dark cycle, and when food was available. Host foraminifera metabolized food to maintain the activity of kleptoplasts and effectively utilized photosynthetic products from both organic and inorganic materials in response to the ambient environment. This suggests that *P. opercularis* behaves as a mixotroph. Simultaneously, kleptoplasts maintain a high intracellular pH environment, indicating that foraminifera capture kleptoplasts not only to gain their photosynthates but also to control the intracellular pH levels to construct a high magnesian calcite test.

Keywords: foraminifera, endosymbiosis, kleptoplasty, protist, ultrastructure, molecular phylogeny

INTRODUCTION

Host–symbiont interactions, for example in endosymbiont-bearing foraminifera, are thought to be a key factor for adaptation and a driving force in evolution (Lee et al., 2010). Foraminifera harbor various endosymbiotic microalgae, including green algae (Chlorophyta), red algae (Rhodophyta), brown algae (Phaeophyta), dinoflagellates (Dinophyta), and diatoms (Diatomea) (Lee et al., 1991). Host foraminifera harbor different symbiotic microalgae as a result of different pathways utilized during foraminiferal evolution. Endosymbiotic microalgae are found only in calcareous foraminifera and may have contributed to their evolution and diversification (Lee et al., 2010). Symbiotic microalgae may support calcification in planktonic foraminifera, as suggested by the observation that treatment with the photosynthesis inhibitor DCMU (3-(3,4-dichlorophenyl)-1,1-dimethylurea) decreased test (shell) growth (Bé et al., 1982). Furthermore, the acquisition of endosymbionts and utilization of the organic materials they produce may enable foraminifera to adapt to an oligotrophic environment. In larger foraminifera, oxygen readily permeates the host cell due to photosynthesis by endosymbiotic algae. Compared with their smaller, nonendosymbiotic counterparts, larger foraminifera can produce more juveniles during asexual reproduction (Röttger, 1974), thus increasing their population size. In this manner, endosymbiosis promotes foraminiferal species diversity and facilitates foraminiferal adaptation to a range of environments.

Algal endosymbionts in foraminifera are considered to have at least two main beneficial roles (Hallock, 1999). The first role is to produce organic materials such as amino acids and glucose via oxygenic photosynthesis, providing the host with resources for growth and reproduction (Hallock, 1981). In turn, symbionts utilize host metabolites (Hallock, 1999). Second, algal endosymbionts contribute to the growth of host foraminiferal tests via calcium carbonate biomineralization (Röttger, 1974). However, the mechanisms underlying the calcification process in foraminiferal cells and how algal endosymbionts contribute to this calcification are unknown. In nonsymbiont-bearing foraminifera, pH changes, calcium ion accumulation and elimination of magnesium ions occur at the calcification site (Toyofuku et al., 2008; de Nooijer et al., 2009), and foraminifera actively change surrounding pH by outward proton pumping and maintaining a wide range of $p\text{CO}_2$ (Toyofuku et al., 2017). The presence of endosymbiotic microalgae in foraminiferal cells may shift their intracellular pH environment toward being more like that of nonsymbiont-bearing foraminifera; consequently, the endosymbiotic contribution to foraminiferal calcification is likely high.

The species of algal endosymbionts in foraminiferal cells differ and affect material cycling between host and symbiont, which has an important role for foraminiferal ecology. Endosymbiotic diatoms of foraminifera lose their frustules and exist in close proximity to the host cytoplasm (Lee et al., 1991; Chai and Lee, 2000). In contrast, endosymbiotic dinoflagellates have distinct plasma membranes (Lee et al., 1991; Hemleben et al., 1989). As a result, the growth rate of the diatom-bearing

foraminifera *Amphistegina lobifera* maintained in phosphate- and nitrate-enriched culture media was higher than that of the dinoflagellate-bearing foraminifera *Amphisorus hemprichii*, which received microalgae as food materials (Lee et al., 1991). It is possible that *A. lobifera* utilizes dissolved organic matter whereas *A. hemprichii* utilizes particulate organic matter. Obviously, the growth rate varies depending on the type of food available and the type of symbiotic algae.

Some species of benthic foraminifera exhibit a particular form of endosymbiosis in which exogenous chloroplasts (so-called kleptoplasts) are retained in the foraminiferal cytoplasm (Lopez, 1979; Bernhard and Bowser, 1999; Bernhard, 2003; Pillet et al., 2011; Tsuchiya et al., 2015; Jauffrais et al., 2016, 2018). Kleptoplasty is a peculiar phenomenon in which heterotrophic organisms capture and maintain exogenous algal chloroplasts (Waugh and Clark, 1986), retaining them essentially as organelles and using their photosynthetic machinery to generate organic materials such as amino acids (Maeda et al., 2012; Tsuchiya et al., 2018). Kleptoplasty occurs in some organisms from protists to metazoans; for example, the dinoflagellate *Dinophysis acuminata* retains plastids of cryptophytal origin (Park et al., 2006), rarely in metazoans, the sea slug *Elysia chlorotica* carries chlorophytal plastids (Rumpho et al., 2000), and the flatworms *Baicallellia solaris* and *Pogaina paranygulgus* retains plastids of diatoms (Van Steenkiste et al., 2019). Among the foraminifera, host organisms maintain kleptoplasts that originated from various species of diatoms (Grzymski et al., 2002; Pillet et al., 2011; Tsuchiya et al., 2015; Chronopoulou et al., 2019; Jauffrais et al., 2019b).

Kleptoplasts within foraminiferal cells retain their photosynthetic machinery in light: the use of ^{14}C -labeled $\text{H}^{14}\text{CO}_3^-$ in an incubation experiment revealed kleptoplastid carbon fixation, as did culture experiments performed under various lighting conditions (Lopez, 1979). Furthermore, host foraminifera retained kleptoplasts longer when they were kept in constant dark rather than constant light (Jauffrais et al., 2016; Cesbron et al., 2017), although carbon assimilation rates were higher in light and varied among species (Lopez, 1979). Carbon and nitrogen assimilation in the foraminiferal cell were obviously occurred (LeKieffre et al., 2018; Jauffrais et al., 2019a). In another study, *Nonionella stella* retained kleptoplasts with intact photosynthetic machinery for as long as 1 year under the low-irradiation conditions below the euphotic zone of the Santa Barbara basin (Grzymski et al., 2002). Three possibilities have been proposed for the function of foraminiferal kleptoplasts under the low levels of light irradiation: photosynthesis under extremely low irradiance level, generation of an electrochemical gradient, and inorganic nitrogen assimilation (Grzymski et al., 2002). Isotope labeling experiment was carried out to understand kleptoplastid functionality both under light and dark conditions (Jauffrais et al., 2019a). Although inorganic carbon assimilation was not occurred, inorganic nitrogen and sulfate assimilations were occurred in both light and dark conditions in aphotic *Nonionella labradorica*. They proposed that the photosynthetic pathways are not functional and possibly to have ammonium and sulfate assimilation pathways (Jauffrais et al., 2019a). However, the mechanisms through which host

foraminifera acquire kleptoplasts, use their photosynthetic products, and genetically activate kleptoplastid photosynthesis are not well understood.

The benthic foraminifera *Planoglabratella opercularis* (d'Orbigny, 1839) is distributed in the intertidal zone of rocky shores, where it crawls on the thalli of coralline algae and grazes on the microalgae and organic detritus on the surface (Kitazato, 1994; Tsuchiya et al., 2014). *Planoglabratella opercularis* has a relatively short life-cycle (approximately 2 months) and is amenable to culture under laboratory conditions (Tsuchiya et al., 1994, 2014). This species has not been reported to harbor endosymbiotic microalgae, alternatively retained kleptoplast (Jauffrais et al., 2018; Tsuchiya et al., 2018).

The aim of the study was to understand the acquisition and maintenance of kleptoplasts in the rocky-shore benthic foraminifera *P. opercularis* and to determine whether kleptoplasty is a key factor for foraminiferal ecology in the metabolic and adaptive mechanisms of this species. To this end, we conducted molecular phylogenetic analyses of both the host foraminifera and the kleptoplasts to understand the origin of the kleptoplasts and whether their presence suggested monophyly within the foraminiferal lineage. In addition, we performed transmission electron microscopy (TEM) to understand the morphology of the kleptoplasts and culture experiments to assess kleptoplastid autofluorescence and the effects of light and food availability on the preservation and digestion of kleptoplasts by the host. Oxygen production and consumption rates were assessed to determine kleptoplastid photosynthetic activity and retention. Finally, we discussed the role of the kleptoplast for calcareous test construction by measuring the intracellular pH.

MATERIALS AND METHODS

Sample Collection and Processing

We collected specimens of *P. opercularis* from the upper to lower intertidal zones of rocky shores at Minami-Izu, Shizuoka Prefecture, Japan (34°36.9'N, 138°49.3'E, 13 July 2011; 21 April, 11 August, 23 Oct 2012); Kamogawa, Chiba Prefecture, Japan (35°07'N, 140°10'E, 4 April 2009); Atsumi, Tsuruoka, Yamagata Prefecture, Japan (38°58'N, 139°55'E, 1 May 2011); and Ofunato, Iwate Prefecture, Japan (39°06'N, 141°52'E, 5 October 2009). These samples were used for molecular phylogenetic analysis and culture experiments. The foraminifera were found on the coralline algae (*Corallina pilulifera*, Rhodophyta) and trapped sediment. Living individual foraminifera were retrieved using a Pasteur pipette under a binocular microscope (SZX7, Olympus Corporation, Tokyo, Japan).

Transmission Electron Microscope (TEM) Observations

We evaluated both the existence and morphology of kleptoplast in the foraminiferal cytoplasm by TEM observation. To compare the intracellular organization of kleptoplasts and various organelles between collected and cultured specimens, we fixed selected specimens from Minami-Izu with glutaraldehyde just

after their collection. Detailed procedures of preparation for TEM observations are provided in Tsuchiya et al. (2015). The TEM analysis was carried out using a JEM-1210 (JEOL Ltd.) and a TECNAI G² 20 (FEI, Hillsboro, OR, United States) at an acceleration voltage of 80 and 120 kV, respectively.

Intracellular pH Imaging

Intracellular pH imaging was carried out by using the fluorescent probe pyranine 8-hydroxypyrene-1,3,6-trisulfonic acid trisodium salt (HPTS) according to the method reported by de Nooijer et al. (2008, 2009). Specimens were cultured with a final concentration of 20 μM HPTS (Sigma-Aldrich) in filtered seawater (0.2-μm pore-size membrane). Intracellular HPTS fluorescence was detected with an inverted fluorescence microscope with phase contrast apparatus (Zeiss, Axio Observer Z1, Carl Zeiss Japan, Tokyo, Japan) for up to 30 min, and then photographed for every 10 s. Calibration and conversion of excitation ratio to actual pH were carried out following de Nooijer et al. (2008).

Molecular Identification

DNA sequencing was conducted to identify the origin of the kleptoplasts. As a host marker, we amplified the internal transcribed spacers (ITS) region of the nuclear ribosomal RNA (*rRNA*) gene using the oligonucleotide primer pair S20 and 2TAIC (Pawlowski, 2000). To distinguish the origin of the kleptoplasts, we amplified the plastid *16S* (*cp16S*) *rRNA* gene using the primer pair PL16S1 and PL16S2 (Takishita et al., 1999). We used the same specimens for both the phylogenetic evaluations based on ITS sequences and the molecular phylogenetic analyses of kleptoplasts.

The amplified PCR products were purified using MonoFas DNA Purification Kit (GL Sciences Inc., Tokyo, Japan), ligated into the pDrive Cloning Vector, and cloned into EZ Competent Cells (Qiagen, Tokyo, Japan) according to the manufacturer's instructions. Plasmids were extracted using the QIAprep Miniprep kit (Qiagen) and sequenced (ABI 3130xl Genetic Analyzer and BigDye Terminator v3.1 Cycle Sequencing Kit, Applied Biosystems, Inc., Foster City, CA, United States). All nucleotide sequences were verified to be free of chimeric sequences using the Bellerophon server (Huber et al., 2004) available online¹ (last accessed Feb 27, 2020). Detailed methods involved in individual sorting, PCR amplification, cloning, and sequencing have been described by Tsuchiya et al. (2000, 2003, 2009, 2015).

The sequences were aligned using ClustalW (Thompson et al., 1994) and corrected manually with the sequence alignment editor Se-Al ver. 2.0a11 (Rambaut, 1996). All major gaps were excluded from the analysis, leaving sequences of approximately 980 nucleotides (nt) for foraminiferal ITS and approximately 715 nt for plastid *16S rRNA* for analyses. To clarify the origin of the kleptoplasts, we used relatively short nucleotide sequences for *16S rRNA* analysis (approx. 715 nt) to reflect the length of known plastid sequences in the GenBank database. Evolutionary trees were reconstructed with the maximum-likelihood method

¹<http://comp-bio.anu.edu.au/bellerophon/bellerophon.pl>

(Felsenstein, 1981) for both datasets. The evolutionary model was calculated using MrModeltest 2.3 (Nylander, 2004), which calculates the best model for DNA evolution according to maximum-likelihood analysis. In addition, the aligned sequences underwent maximum-likelihood analysis using a general time-reversible (GTR) model (Rodriguez et al., 1990) with correction for the proportion of invariable sites (I) and for the rate of variation among sites for a gamma distribution shape parameter (Γ) as implemented in PhyML 3.0 (Guindon et al., 2010). For Bayesian inference, we used MrBayes (Huelsenbeck and Ronquist, 2001) with the GTR+I+ Γ model. Markov-chain Monte Carlo (MCMC) simulation was applied to approximate the posterior probabilities (PPs) of trees for MrBayes that were constructed according to 50% majority-rule consensus after the exclusion of burn-in trees. The MCMC simulation in MrBayes was run with one cold and three heated chains for 1,000,000 generations. Log-likelihood and branch length were sampled every 100 generations to yield the PPs for each data set.

Bootstrapping was conducted with 100 replicates for maximum-likelihood analysis. We used *Angulodiscorbis quadrangularis* (AF498326) as an outgroup for the analyses of host foraminiferal ITS, which are closely related to those of planoglabratellid species (Tsuchiya et al., 2000, 2003), and *Bolidomonas mediterranea* (AY702144) as an outgroup for the analyses of plastid *16S rRNA* gene sequences, which show ancestral lineages of diatom species (Guillou et al., 1999). The sequences obtained in this study have been deposited in the GenBank database (accession numbers: KP792453–KP792510).

Observation of Kleptoplastid

Autofluorescence

Culture Experiments and Observation of Autofluorescence

The specimens of *P. opercularis* for the culture experiments were rinsed with filter-sterilized seawater (0.2- μm pore-size membrane) and cleaned with a fine writing brush to remove any associated microorganisms on the test surface. In order to avoid differences in fluorescence depending on the growth stage of individual specimens, we used individual specimens with an average of 22.6 ± 5.5 chambers. Live specimens were maintained in a small culture dish with 15 ml of filter-sterilized seawater. All cultures were maintained in an incubator at 20°C, the optimal temperature for *P. opercularis* (Tsuchiya et al., 1994, 2014); salinity and pH were 34 and 8.17, respectively. To keep the salinity and pH constant, we changed the seawater every 2 days. The light intensity was measured by using a Quantum PAR (photosynthetically active radiation) meter (MQ-200, Apogee Instruments, Inc., Logan, UT, United States). During the culture period, we confirmed the color of the foraminiferal cells at the same time as observing autofluorescence and pseudopodial activity, and obtained photographs using an inverted microscope with a phase-contrast apparatus (Axio Observer D1) before and at the end of the culture experiment to determine qualitative indices for foraminiferal activity (data not presented in this study).

To determine the influences of both food availability and light conditions on the retention of kleptoplasts, we conducted culture experiments with and without food materials under various conditions of light intensity and irradiation time as described detail below, and measured the intensity of kleptoplastid autofluorescence as the qualitative index for chlorophyll. Chlorophyll fluorescence does not directly indicate the functionality of photosynthetic activity. However, this method is also useful for revealing kleptoplast dynamics in multiple specimens. The autofluorescence of individual specimens was measured using a binocular microscope with epifluorescence apparatus (U-RFL-T, Olympus) and was recorded using a digital camera with a constant exposure time of 0.4 s; we used the ImageJ software ver. 1.51a (Schneider et al., 2012, NIH, Washington, DC, United States) to determine the intensity of autofluorescence in arbitrary units (A.U.). Autofluorescence as a function of density of kleptoplasts varies among specimens in nature. We therefore measured the average relative intensity (R.I.) of autofluorescence on each measurement day during the culture period; we defined the intensity of autofluorescence on the first day of the culture experiment as 100% for all experimental groups. We noted that autofluorescence varied over time; therefore, to determine whether autofluorescence differed significantly between experimental groups or time points, we conducted two-way ANOVA and *t*-tests to compare the five experimental groups that assessed the influence of food availability and the four experimental groups that evaluated the influence of lighting conditions.

Selected specimens from each time series were fixed in 2.5% filtered seawater-buffered glutaraldehyde for observation under TEM. The culture conditions with respect to food availability and light and the number of individual specimens in each experimental group are shown in **Table 1**.

Influence of Food Availability on Autofluorescence

We evaluated kleptoplastid autofluorescence under five different conditions of food availability to determine the effect of food availability on kleptoplastid retention. Cultures were incubated for 11 days under a 12:12-h light:dark cycle with 5 different combinations of food sources and feeding durations (**Table 1**): (1) no food provided; (2) heat-killed (microwaved) *Chlorella* cells added throughout the culture period; (3) heat-killed *Chlorella* cells provided during the first 2 days of culture only; (4) live *Chlorella* cells added throughout the culture period; and (5) live *Chlorella* cells added during the first 2 days only. In order to reveal acquisition and maintenance of kleptoplasts from diatoms through TEM observation, it is necessary to distinguish the retained diatom-derived kleptoplasts from the food. In addition, we used *Chlorella* cells as a food source in order to examine whether other microalgal-derived chloroplasts have the potential to be used for kleptoplasts. All other conditions—water temperature, salinity, pH, and light intensity (30 $\mu\text{mol photon m}^{-2} \text{ s}^{-1}$ PAR)—were held constant. The light intensity was equivalent to that at a 3-m water depth at the sampling site. *Chlorella* sp. cells were originally supplied by the Biological Institute of the University of Tübingen (Germany) and were subsequently grown in our laboratory (Heinz et al., 2001). To

TABLE 1 | Food source and availability and light conditions in culture experiments.

Food condition	Light condition	No. of specimens		Notes
		at start	at end	
—	—	10	—	Natural abundance
A. No food	12:12-h light:dark	30	25	Influence of food availability
B. Heat-killed <i>Chlorella</i> cells for 11 days	12:12-h light:dark	15	14	
C. Heat-killed <i>Chlorella</i> cells for first 2 days only	12:12-h light:dark	15	14	
D. Live <i>Chlorella</i> cells for 11 days	12:12-h light:dark	15	13	
E. Live <i>Chlorella</i> cells for first 2 days only	12:12-h light:dark	15	14	
F. No food	Constant dark	45	38	Influence of light condition
G. No food	24:24-h light:dark	30	29	
H. No food ^a	12:12-h light:dark	30	25	
I. No food	Constant light	45	30	

^aSame as a.

keep concentration of the *Chlorella* cells constant, we changed the seawater every two days, and were kept approximately 4.3×10^4 cells/mL for each fed group. Live but not heat-killed *Chlorella* cells displayed autofluorescence, whereas heat-killed *Chlorella* cells did not show autofluorescence. We distinguished autofluorescence of kleptoplast within foraminiferal cells from ambient autofluorescence of *Chlorella* cells using ImageJ, and extracted only kleptoplastid autofluorescence in the foraminiferal cell from captured images.

Influence of Lighting Condition on Autofluorescence

To understand the influence of irradiation time on the retention of kleptoplasts, cultures were maintained for 11 to 14 days without food materials and under varied conditions of irradiation time (**Table 1**): (1) 24-h dark condition; (2) 24:24-h light:dark cycle; (3) 12:12-h light:dark cycle; and (4) 24-h light condition. All other conditions were held constant, as described earlier.

Kleptoplastid Oxygen Production

Assessment of Respiration and Oxygen Production

To characterize the photosynthetic activities of kleptoplasts, we used freshly collected specimens and measured the oxygen consumption in different areas of foraminiferal cells as an index of respiration rates of the specimen under constant light condition using an oxygen microsensor (OX-25, Unisense A/S Aarhus N, Denmark) connected to a Microsensor Multimeter (Unisense A/S) (**Supplementary Figure S1A**). We used an aeration device to maintain the dissolved oxygen (DO) concentration in the aquarium. Prior to measurement, we conducted two-point calibrations of the system under conditions of both undersaturation and saturation of DO concentration with nitrogen gas (0% O₂) and aeration with a pump (100% O₂), respectively. We used a horizontal binocular microscope (Kitazato, 1984) attached to the aquarium to check the position or angle of a foraminifer in the capillary tube. The aquarium was exposed a maximum light intensity of $320\text{-}\mu\text{mol photon m}^{-2} \text{ s}^{-1}$ PAR, which is equivalent to that at the sea surface (0 m water depth) at the sample collection site. The sensor tip (diameter, 20–30- μm) of the

oxygen microsensor was inserted into a small capillary tube (inner diameter, 0.36 mm; inner height, 3 mm; volume; $0.97 \mu\text{L}$) prepared in our laboratory and placed in an aquarium (160 mm \times 160 mm \times 160 mm) filled with filtered seawater (water temperature: 21.4°C, salinity: 33.8) (**Supplementary Figure S1B**). Measurements began 500 μm above the top edge of the capillary tube and were collected at 50- μm intervals to 3 μm above the specimen. The oxygen consumption rates were calculated using the MicOx software (Unisense A/S²).

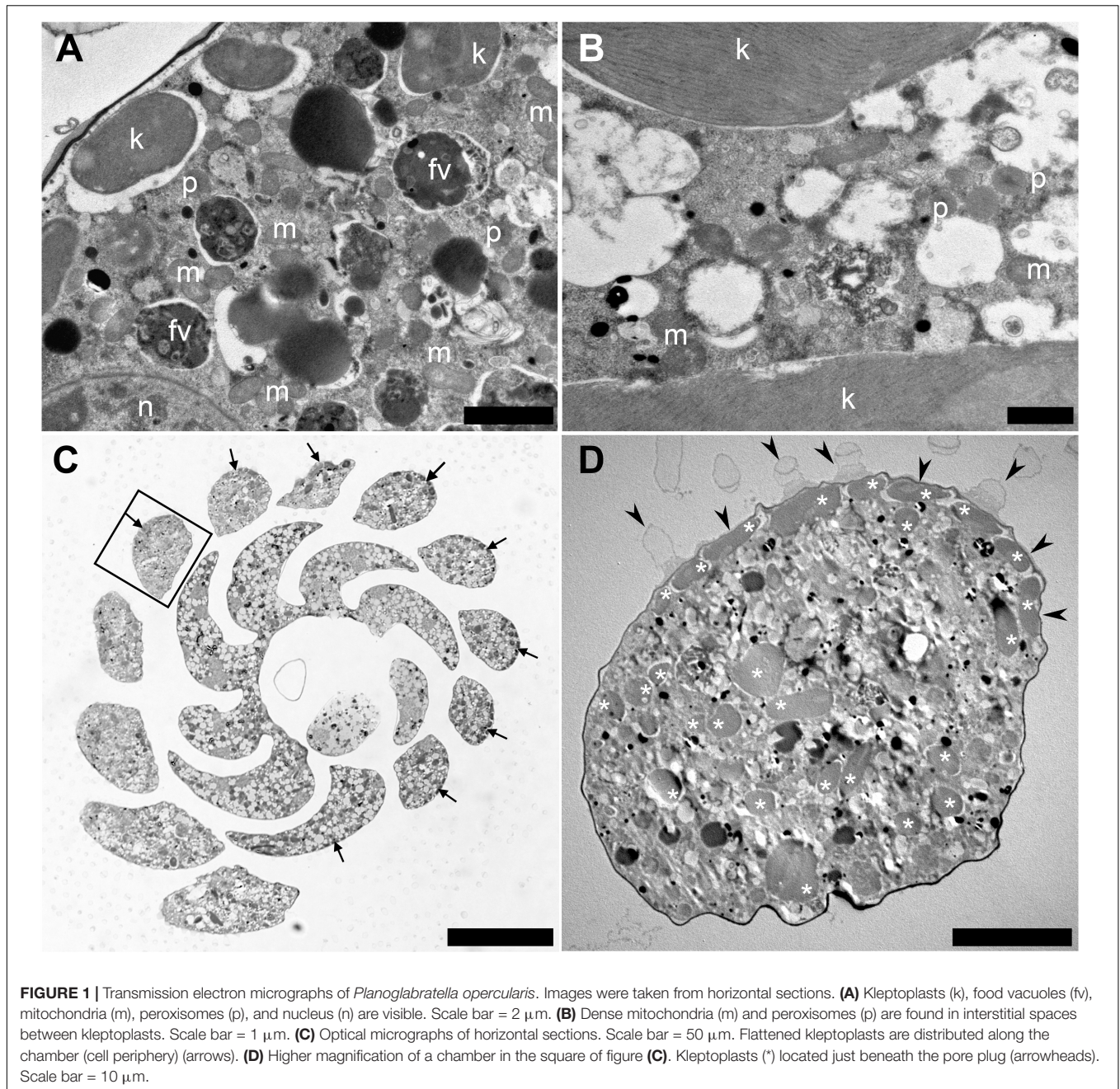
Response of Oxygen Production to Light Intensity

To measure the respiration rate of individual specimens, we used freshly collected specimens and used a small capillary tube with an oxygen microsensor, as described earlier in the Methods, to characterize how oxygen production responds to changes in light intensity (**Supplementary Figure S1B**). We measured the rate of respiration at different sites (dorsal, ventral, and lateral sides) of individual foraminiferal cells in light because the pore size and pore density of the test of foraminifera changes with the ambient environmental conditions, presumably to adjust gas exchange (Moodley and Hess, 1992).

We also measured oxygen production at varying light intensities of 0, 7, 33, and 320 $\mu\text{mol photon m}^{-2} \text{ s}^{-1}$ by placing a microsensor 3 μm above the dorsal side of the specimen. For both of these measurements, the oxygen concentration was measured by using a MicroProfiling System (Unisense A/S) in which the microsensor was controlled by the Sensor Trace PRO software (Unisense A/S).

To assess whether respiration and oxygen production were balanced, we used a MicroRespiration Chamber (Unisense A/S) as described in the previous section to measure the bulk respiration rate of individual specimens (**Supplementary Figure S1C**). We measured oxygen production and respiration in the absence of food materials in 5 individual specimens

²<http://www.unisense.com/>



under light conditions ($320\text{-}\mu\text{mol photon m}^{-2} \text{s}^{-1}$) or in the dark.

RESULTS

Kleptoplast Morphology

Configuration and Localization of Kleptoplasts

To understand the acquisition and maintenance of kleptoplasts in the rocky-shore benthic foraminifera *P. opercularis* and to determine whether kleptoplasty is a key factor for foraminiferal ecology in the metabolic and adaptive mechanisms of this

species, we observed that the cytoplasm of *P. opercularis* contained kleptoplasts (**Figure 1A**), but kleptoplastid division was not observed. The kleptoplasts were clearly distinguishable from food materials (**Figure 1A**) and algal symbionts. The digestive vacuoles of freshly collected specimens contained food materials with indistinct structures (**Figure 1A**). Mitochondria and peroxisomes were frequently present around kleptoplasts (**Figure 1B**). Kleptoplasts were localized along the periphery of the cell (**Figure 1C**), not only on the dorsal side, which is distinguishable in vertical sections of the specimens (Jauffrais et al., 2018), but also accumulated in the outermost chambers of the cell periphery visible in horizontal sections, could not found

outer periphery of the inner whorl (Figure 1C). Kleptoplasts were distributed just beneath the cell membrane, with the highest density at the cell periphery (Figure 1D), where light intensity was highest. Kleptoplasts just beneath the pore plug were flattened (Figure 1D).

The density of kleptoplasts differed between areas within each chamber, and kleptoplasts were distributed heterogeneously throughout the chambers in freshly collected specimens (Figure 2A). However, distribution pattern of this heterogeneity varied from specimen to specimen—one specimen collected from the same location at the same time showed a homogeneous distribution of kleptoplasts and cytoplasm throughout the chambers (Figure 2B), which were separated by plugs, while another specimen showed homogeneous distribution of both kleptoplasts and cytoplasm without plugs (Figure 2C). The specimen with heterogeneous distribution of kleptoplasts had at least three distinct features (Figures 2D–F). First, a number of the vacuoles in the first few chambers were found from the initial chamber at the apex of the test. Kleptoplasts were associating with these vacuoles (Figure 2D). Second, a high abundance of kleptoplasts with small number of vacuoles was present in the middle of the trochospiral chambers (Figure 2E). Third, a few kleptoplasts with abundant vacuoles were present in the last few chambers of the last trochospiral whorl (Figure 2F). Food materials were visible throughout the chamber at the first two sites, but digestive residues were found at the third site.

We confirmed kleptoplastid autofluorescence in asexually reproducing juveniles (Supplementary Figure S2). Just after the reproduction, three-chambered juveniles show autofluorescence, although the third chamber does not have autofluorescence (Supplementary Figures S2A,B). In the four-chambered juvenile, autofluorescence was still present two days after reproduction (Supplementary Figures S2C,D). However, individual specimen lacked cytoplasm color, and showed weak autofluorescence after 5 days (Supplementary Figures S2E,F). After addition of diatom cells, the five-chambered individual specimen captured the diatom cells with pseudopodia, and autofluorescence was recovered (Supplementary Figures S2G,H). During this period, neither cytoplasm color nor autofluorescence was detected in the last chamber (Supplementary Figure S2H). After 10 days (two days after in addition of diatom cells), we detected brownish-colored cytoplasm and autofluorescence in all chambers (Supplementary Figures S2I,J).

Kleptoplast Variability Over Time

Using its pseudopodia, *P. opercularis* captured live diatoms at the ventral aperture (Supplementary Figure S3), leaving behind the diatom frustules. In unfed cultures, kleptoplasts were present throughout the experimental period but degraded with time (Supplementary Figures S4A–D). On the first day of culture, distinct kleptoplastid structures and food materials were observed in the vacuoles (Supplementary Figures S4A,B). On day 2, some kleptoplasts were located in the vacuoles and developed spaces between the lamellae (Supplementary Figures S4C,D). Kleptoplastid degradation increased over the 11 days in unfed cultures (Supplementary Figures S4E,F). There

were numerous lipid droplets in the cytoplasm (Supplementary Figure S4E) and digestion of kleptoplastid residues could be seen (Supplementary Figure S4F).

Acquisition of *Chlorella* Chloroplast

In the experimental group fed heat-killed *Chlorella* during the culture period, kleptoplastids still had both the thylakoid and the chloroplast membranes on day 2 (Supplementary Figures S5A,B) and presumed *Chlorella* cells in the food vacuoles (Supplementary Figure S5B). However, by day 11, both food materials and kleptoplasts were digested (Supplementary Figures S5C–F) and the kleptoplastid outer membrane (Supplementary Figures S5C,E) and those of thylakoid membranes were degraded (Supplementary Figure S5F).

In the cultures fed live *Chlorella* during the experimental period, both kleptoplasts and their envelopes were intact on day 2, as was seen in the other experimental groups (Supplementary Figures S6A,B). However, some kleptoplasts were still present, and kleptoplastid membranes were degraded on day 11 (Supplementary Figures S6C,D).

Interestingly, by day 11, live *Chlorella* chloroplasts seemed to have established a kleptoplastic relationship with the host foraminifera (Figure 3), although *Chlorella* chloroplasts were not noted on day 2 (Supplementary Figures S6A,B). Specifically, intracellular chloroplasts of *Chlorella* lacked not only a cell wall, but also a cytoplasm (Supplementary Figures S6C–E), which remained the cell wall in the vacuole, and an accumulation of mitochondria was seen (Supplementary Figure S6F). Like the diatom chloroplasts that give rise to kleptoplasts in *P. opercularis*, the captured *Chlorella* chloroplasts present in host vacuoles had distinct thylakoids and starch granules (Figure 3B; Supplementary Figure S6E) and were located not only within host foraminiferal cells but also along the cell periphery. In particular, some of the captured *Chlorella* chloroplasts were observed just beneath the pore plug (Figure 3B), as were the kleptoplasts (Figure 1D). However, like the kleptoplasts, intracellular *Chlorella* did not appear to undergo cell division in host foraminiferal cells.

Molecular Phylogenetic Analyses

Molecular Phylogenetic Analyses of the Host Foraminiferal ITS

We obtained a total of 17 foraminiferal ITS sequences (13 sequences for genotype A and 4 sequences for genotype B) from 8 individual specimens. The sequences were 99% homologous to *P. opercularis* genotype A (AF498340) and *P. opercularis* genotype B (AF498351) among the planoglabratellid species, with high posterior probabilities (Supplementary Figure S7). The topology of the Bayesian phylogenetic and maximum-likelihood trees yielded nearly the same phylogenetic relationships.

Molecular Phylogenetic Analyses of Plastid 16S rRNA

We obtained 73 kleptoplastid 16S rRNA sequences from 14 individual specimens. The obtained sequences were originated from various diatom chloroplasts, no other microalgal chloroplasts, 96–99% homologous to those from

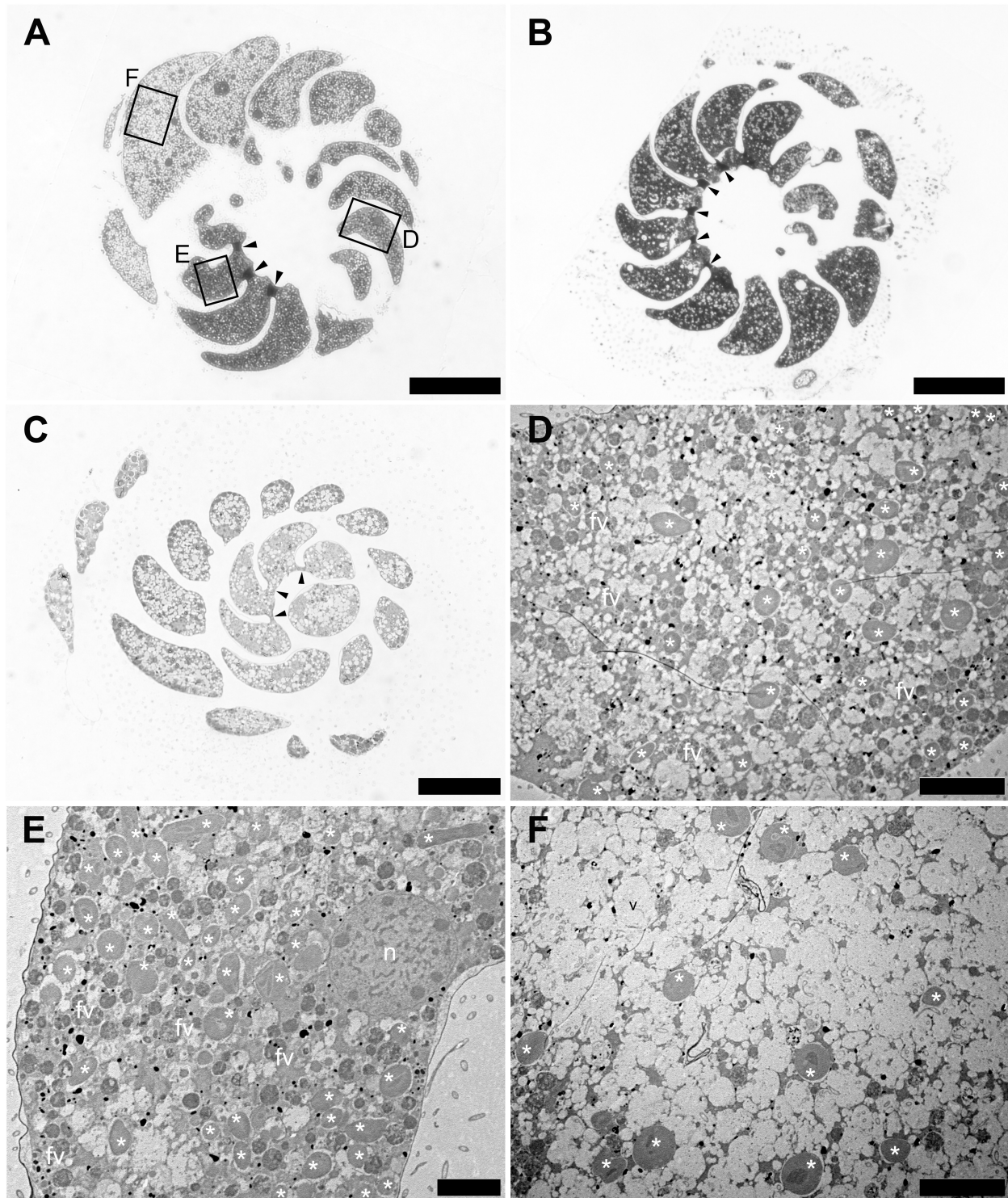
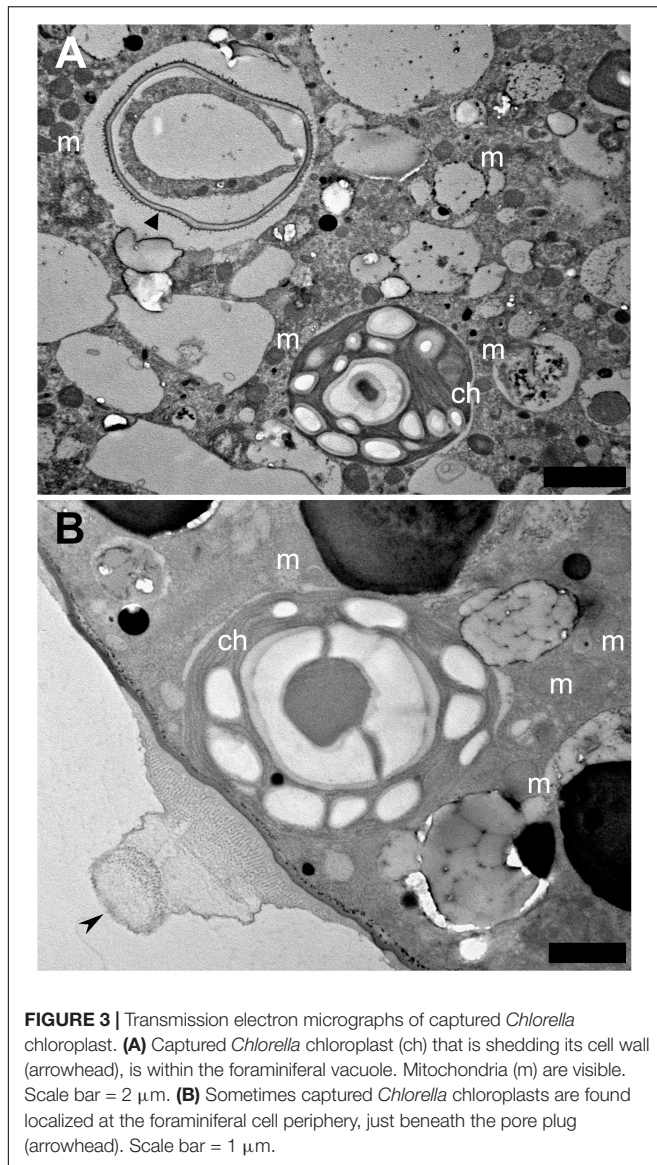


FIGURE 2 | Optical and Transmission electron micrographs (TEMs) of *Planoglabratella opercularis*. **(A)** Heterogeneous features of cytoplasm between chambers are separated by plugs (arrowheads). Squares indicate regions featured in the indicated panels of figures **(D–F)**. Scale bar = 100 μm . **(B)** Homogeneous features of cytoplasm among chambers that are separated by plugs (arrowheads). Scale bar = 100 μm . **(C)** Homogeneous features of cytoplasm among chambers that lack plugs between chambers (arrowheads). Scale bar = 50 μm . **(D–F)** Higher Magnification TEMs, which are indicated as squares in figure **(A)**. **(D)** Kleptoplasts (*), food vacuoles (fv), and vacuoles are visible. Scale bar = 10 μm . **(E)** Kleptoplasts (*) and food vacuoles (fv) are densely distributed. Scale bar = 5 μm . **(F)** Numerous empty vacuoles are distributed throughout the chamber and a few kleptoplasts (*) are visible. Scale bar = 10 μm .



Amphora spp. [*Amphora* sp. C10 (FJ002217), *A. ovalis* (EU580470), *A. coffeaeformis* (FJ002183)], 94–98% homologous to *Phaeodactylum tricornutum* (EF067920), 97–99% identical to *Navicula* sp. C20 (FJ002226), 96–98% homologous to pennate diatom sp. CCAP 1008/1 (FJ002185), and 96–97% similar to *Cylindrotheca closterium* (FJ002223), all of which are Bacillariophyceae diatoms. In addition, a single sequence showed 97% similarity to *Nanofrustulum shiloi* (FJ002232), a Fragilariophyceae diatom.

Phylogenetic analysis showed that the sequences clustered with *Amphora* species and *Nitzschia closterium* (FJ002221) with high posterior probability (PP) values (Figure 4). Several sequences were closely related to *Fragilariopsis cylindrus* (FJ002238), with relatively high PPs. Although the associated PP values were not robust, one closely related nucleotide sequence clustered with *Fragilaria* and *Navicula* species. Because the nucleotide sequences were fairly short (715 nt), the diatom

species from which some nucleotide sequences were obtained could not be determined.

Fluctuation of Kleptoplastid Autofluorescence

Intensity of Autofluorescence Within the Cytoplasm

Influence of food source availability

Kleptoplastid autofluorescence varied according to the availability and type of food provided (Figure 5A and Supplementary Figures S8A, S9A). The autofluorescence was constantly high in the experimental groups that were fed heat-killed *Chlorella* during the culture period or for the first two days only. Interestingly, the R.I. of kleptoplast autofluorescence markedly increased on day 2 (245% and 232%) in both the experimental group that was fed heat-killed *Chlorella*. It gradually decreased thereafter until the end of the culture period, but the intensity of autofluorescence on day 11 was still higher than that on day 0 (100%), especially for groups fed heat-killed *Chlorella* for the first two days only (83%). The autofluorescence on day 11 fell below that on the first day of culture in the experimental group fed heat-killed *Chlorella* during the culture period (65%).

On the other hand, the mean R.I. of autofluorescence gradually decreased during the culture period in the unfed experimental group and two experimental groups that were fed live *Chlorella* (Figure 5A and Supplementary Figures S8A, S9A). The autofluorescence on day 11 was clearly less than that on day 0 both for the unfed experimental group (19%) and for the groups fed live *Chlorella* for the first two days only (15%). Autofluorescence in the experimental group fed live *Chlorella* throughout the culture period followed a different pattern than that seen in the groups fed heat-killed *Chlorella* or the first two days only or not fed at all. At first, autofluorescence gradually decreased over the first 5 days, as seen in the unfed experimental group, but recovered to more than 60% of the initial level on days 6 and 10. Autofluorescence on day 11 (52%) was still lower than that on day 0. Results of statistical analyses are shown in Supplementary Figures S8A, S9A.

Influence of light conditions

The kleptoplastid autofluorescence varied with light conditions (Figure 5B and Supplementary Figures S8B, S9B). In host foraminifera under constant dark conditions, the mean R.I. of kleptoplastid autofluorescence remained fairly high throughout the 14-day culture period, gradually decreasing by day 8, when it was 69% of the initial level, and then remaining stable at 74% on day 14. Autofluorescence under the 24:24-h light:dark condition showed a similar overall pattern to that under constant dark conditions, remaining fairly high until it fell below the initial level at the end of the culture period (37%).

In comparison, kleptoplastid autofluorescence under 12:12-h light:dark cycle fluctuated during the culture period but tended overall to be attenuated. In particular, the autofluorescence intensity increased from day 2 to day 4 and then sharply decreased.

The R.I. of autofluorescence under constant light decreased markedly from the start of the experiment to day 10. Thereafter,

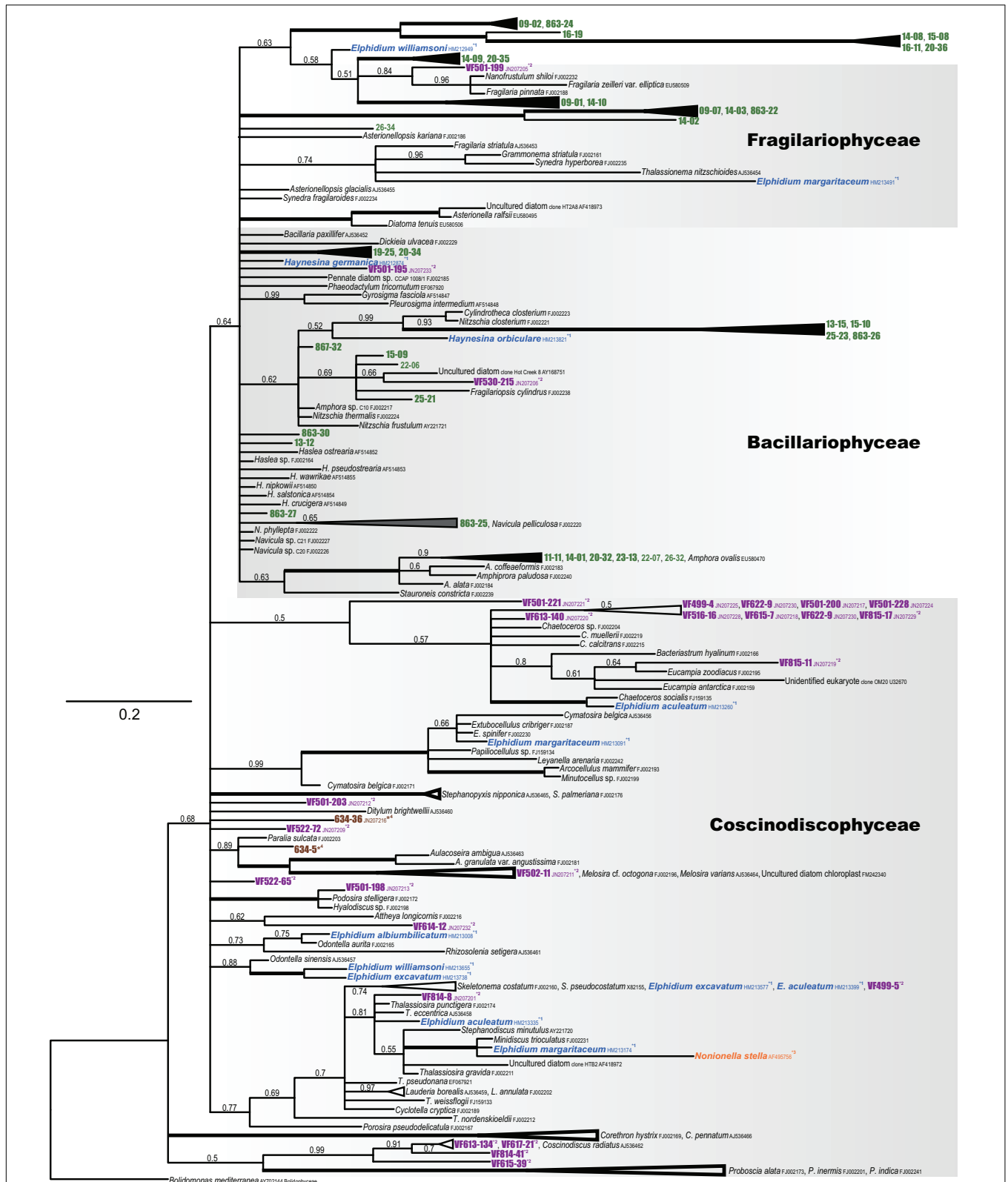
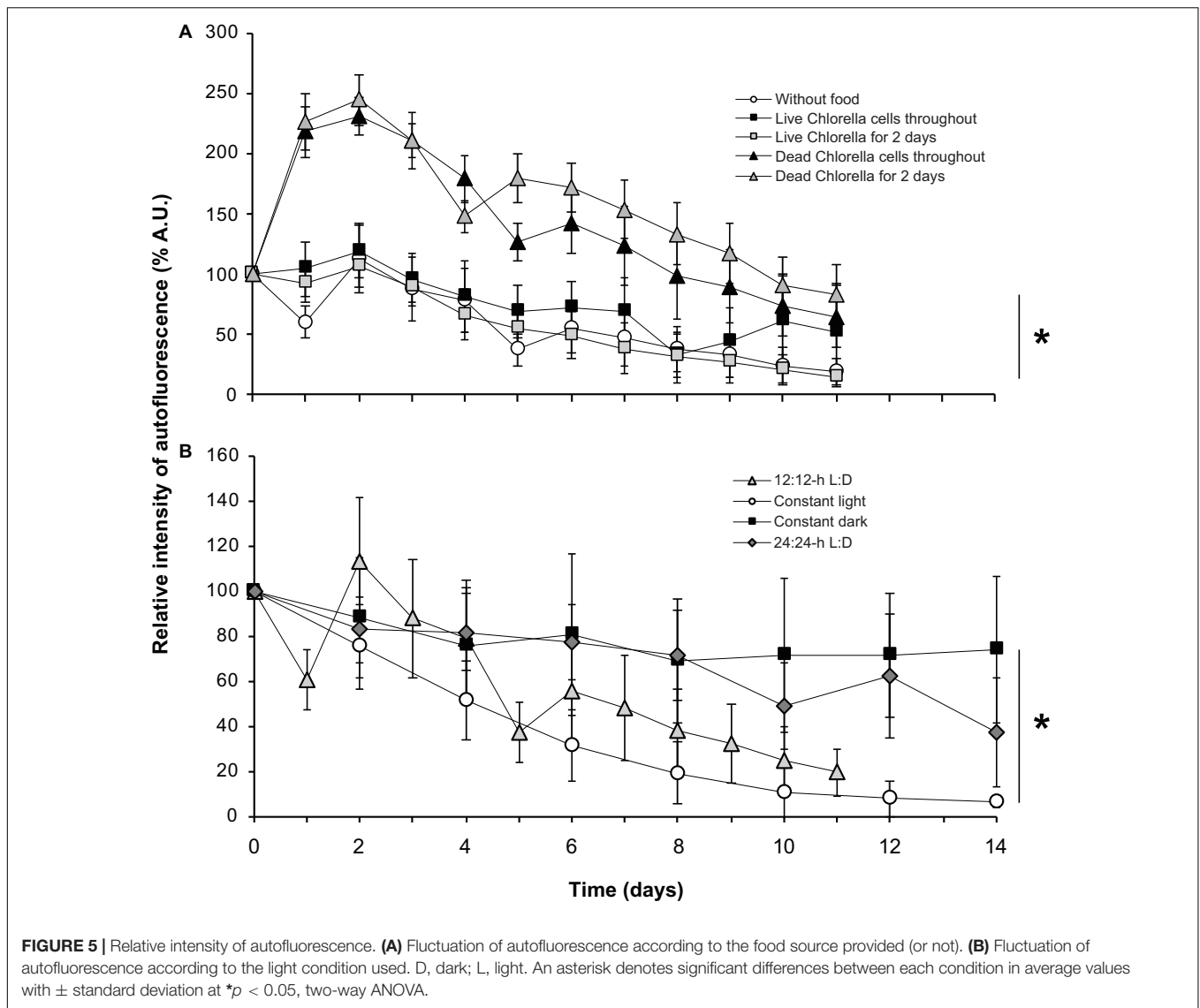


FIGURE 4 | Phylogenetic tree of plastid 16S rRNA (diatom) based on Bayesian inference (MrBayes). Numbers above the internal branches at the nodes indicate the posterior probabilities. Accession numbers follow the species names. *Bolidomonas mediterranea* (AY702144) was used as the outgroup. Kleptoplasts of *P. opercularis* are shown in green; reference kleptoplasts of *Virgulina fragilis* (purple), *Elphidium* species, *Haynesina* species (blue), *Nonionella stella* (orange), and environmental DNA (brown) are also indicated.



it remained at approximate 10% of the initial level and was 6% of the initial level at the end of the culture period. Results of statistical analyses are shown in **Supplementary Figures S8B, S9B**.

Respiration and Oxygen Production

Under constant light, the specimen respiration rates varied markedly from area to area (**Table 2** and **Figure 6**). The mean oxygen concentration just above the dorsal side of a

specimen was $345 \mu\text{mol O}_2 \text{ L}^{-1}$ (**Figure 6A**), while the background oxygen concentration was $227 \mu\text{mol O}_2 \text{ L}^{-1}$, indicating higher oxygen production above the dorsal side. Under these conditions, the rate of oxygen production at the dorsal side was $35.7 \text{ nmol O}_2 \text{ hr}^{-1} \text{ cm}^{-2}$. In contrast, the oxygen concentrations were 149 and $196 \mu\text{mol O}_2 \text{ L}^{-1}$ just above the ventral sides of two individual specimens that were placed upside down in the capillary tube, indicating oxygen consumption, when compared to the background oxygen concentration ($224 \mu\text{mol O}_2 \text{ L}^{-1}$) (**Figures 6B,C**). Accordingly, the rate of oxygen production was -22.9 and $-8.7 \text{ nmol O}_2 \text{ hr}^{-1} \text{ cm}^{-2}$, respectively, which implies that foraminifera consume oxygen at the ventral side. When measured at the lateral side of a specimen, the oxygen concentration was $227 \mu\text{mol O}_2 \text{ L}^{-1}$ compared with the background oxygen concentration of $226 \mu\text{mol O}_2 \text{ L}^{-1}$, yielding an oxygen production rate of $1.0 \text{ nmol O}_2 \text{ hr}^{-1} \text{ cm}^{-2}$ and thus indicating that the respiration of an individual

TABLE 2 | Relationship between light intensity and oxygen production at the test surface.

	A	B	C	D	E
Intensity of light quantum ($\mu\text{mol/m}^2/\text{s}$)	320	0	7	33	320
^aDO concentration ($\mu\text{mol/L}$)	350	259	281	327	331

A–E indicated the timing of light on or light off. ^aDO Dissolved oxygen.

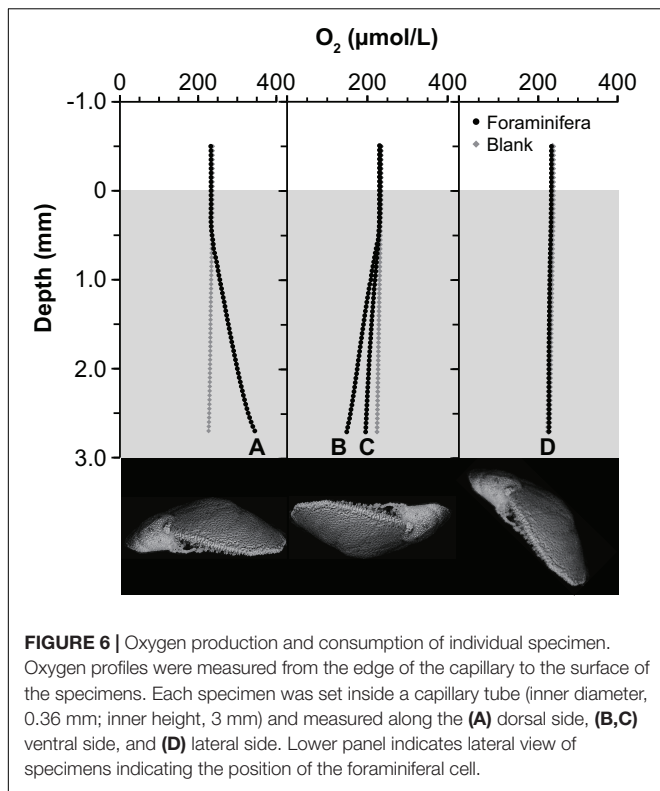


FIGURE 6 | Oxygen production and consumption of individual specimen. Oxygen profiles were measured from the edge of the capillary to the surface of the specimens. Each specimen was set inside a capillary tube (inner diameter, 0.36 mm; inner height, 3 mm) and measured along the (A) dorsal side, (B,C) ventral side, and (D) lateral side. Lower panel indicates lateral view of specimens indicating the position of the foraminiferal cell.

specimen is well-balanced in terms of oxygen production and consumption (Figure 6D).

We measured the overall balance between the oxygen production and respiration rates (that is, gross photosynthesis) in 5 specimens over one hour. The mean oxygen consumption rate was $1.78 \text{ nmol O}_2 \text{ h}^{-1} \text{ 5 individual}^{-1}$ ($0.36 \text{ nmol O}_2 \text{ h}^{-1} \text{ individual}^{-1}$) under constant light compared with $3.31 \text{ nmol O}_2 \text{ h}^{-1} \text{ 5 individual}^{-1}$ ($0.66 \text{ nmol O}_2 \text{ h}^{-1} \text{ individual}^{-1}$) under constant darkness.

Kleptoplastid oxygen production was highly variable and responded promptly to differences in light intensity (Table 2 and Figure 7). The oxygen concentration was $350 \mu\text{mol O}_2 \text{ L}^{-1}$ at a light intensity of $320 \mu\text{mol photon m}^{-2} \text{ s}^{-1}$ at $3 \mu\text{m}$ above the dorsal side of the host (Figure 7A). Immediately after taking the measurement under light conditions, we shifted specimen to dark conditions. After just 5 min in darkness, the oxygen concentration above the dorsal side had decreased markedly, to $259 \mu\text{mol O}_2 \text{ L}^{-1}$ (Figure 7B). The oxygen concentration increased in a step-by-step manner with stepwise increases in light intensity (Figures 7C,D). However, even after prolonged exposure (12 min) to $33 \mu\text{mol photon m}^{-2} \text{ s}^{-1}$, the oxygen concentration reached $327 \mu\text{mol O}_2 \text{ L}^{-1}$, and $331 \mu\text{mol O}_2 \text{ L}^{-1}$ at $320 \mu\text{mol photon m}^{-2} \text{ s}^{-1}$ (Figure 7E). Therefore, oxygen production failed to match the level achieved initially at $320 \mu\text{mol photon m}^{-2} \text{ s}^{-1}$. Note that oxygen production did not reach saturation during this time; rather, there seems to be an oxygen production threshold between 33 and $320 \mu\text{mol photon m}^{-2} \text{ s}^{-1}$ light intensity: oxygen production was similar despite a 10-fold difference in light intensity.

Intracellular pH Condition

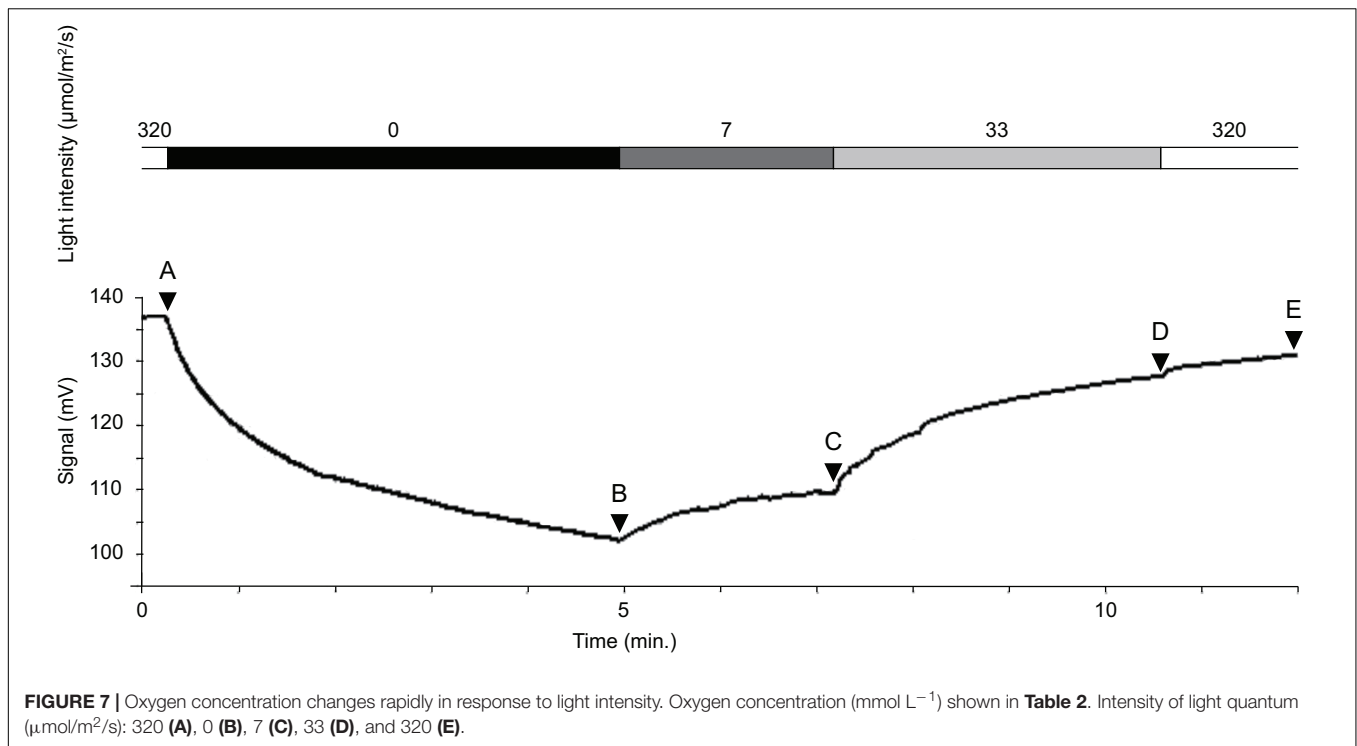
Intracellular pH conditions were different between two specimens of kleptoplast-bearing *P. opercularis* in light condition (Figure 8 and Supplementary Figure S10). Higher pH (7.33 and 7.90 in average) was found in the final chamber of the foraminiferal cell, compared to lower pH (6.63 and 6.64 in average) at center of the cell.

DISCUSSION

Origin of the Kleptoplasts in *P. opercularis*

Using TEM, we found kleptoplasts in the cytoplasm of *P. opercularis*, confirming that the origin of the autofluorescence of *P. opercularis* is solely due to the presence of kleptoplasts (Figures 1,2). Overall morphological features are described in a study by Jauffrais et al. (2018). Kleptoplastid structures are similar to those found in heterokonts and closely resembled the characteristics of kleptoplasts in other foraminifera, such as *Elphidium* species (Lopez, 1979) and *N. stella* (Grzymski et al., 2002), especially those harboring kleptoplasts from Bacillariophyceae diatoms (Bedoshvili et al., 2009; Jauffrais et al., 2018). These findings were congruent with our molecular phylogenetic analysis (Figure 4). For most of the kleptoplast-bearing foraminifera for which nucleotide sequence data have been reported [*Elphidium* species (Pillet et al., 2011) and *N. stella* (Grzymski et al., 2002), *Elphidium* sp. genotype S5, *Ammonia* sp. genotype T6, and *Haynesina* sp. genotype S16 (Chronopoulou et al., 2019), *Elphidium williamsoni* (Jauffrais et al., 2019b), and *Nonionellina labradorica* (Jauffrais et al., 2019a)], the kleptoplasts consistently originated from diatoms, rather than from green algae or dinoflagellates (Correia and Lee, 2000, 2002a). Unlike *N. labradorica*, *P. opercularis* acquired kleptoplasts from various diatom species as reported in *Elphidium* spp. and *Ammonia* sp. (Chronopoulou et al., 2019; Jauffrais et al., 2019b). They confirmed nuclear 18S rRNA sequences in the foraminiferal cell that indicate food variability including diatom.

Planoglabratella opercularis retained kleptoplasts from multiple diatom species (Figure 4), especially epiphytic freshwater, brackish and marine diatoms (Sawai, 2001), consistent with its habitat of crawling on the thalli of coralline algae and grazing on microalgae on the surface of seaweeds (Kitazato, 1994). The foraminiferal specificity for diatoms is not high. In addition, according to the molecular phylogenetic analysis, the diatom species from which the origins of kleptoplasts varied between specimens and differed according to the season during which the sample was collected, the collection location, and other features of the ambient environment of the foraminiferal habitat (Figure 4). In contrast, the kleptoplasts in *Elphidium* species (Pillet et al., 2011) and *Virgulinea fragilis* (Tsuchiya et al., 2015) retained kleptoplasts from planktonic as well as epiphytic diatom species. There is no evidence that *P. opercularis* retain green algal chloroplasts like *Chlorella* cells and other microalgal chloroplasts in natural environments. We have not sequenced nuclear 18S rRNA of diatoms and could



not directly compare between *18S* and *16S rRNAs*. At least, we could not find any nucleus other than those of foraminifera in the TEM observations. Chronopoulou et al. (2019) and Jauffrais et al. (2019a,b) showed nuclear *18S rRNA* sequences of diatoms in the foraminiferal cell. These are important observations to understand acquisition and maintenance of kleptoplasts. Further studies are needed to confirm nuclear *rRNA* sequences of diatoms within *P. opercularis* cell.

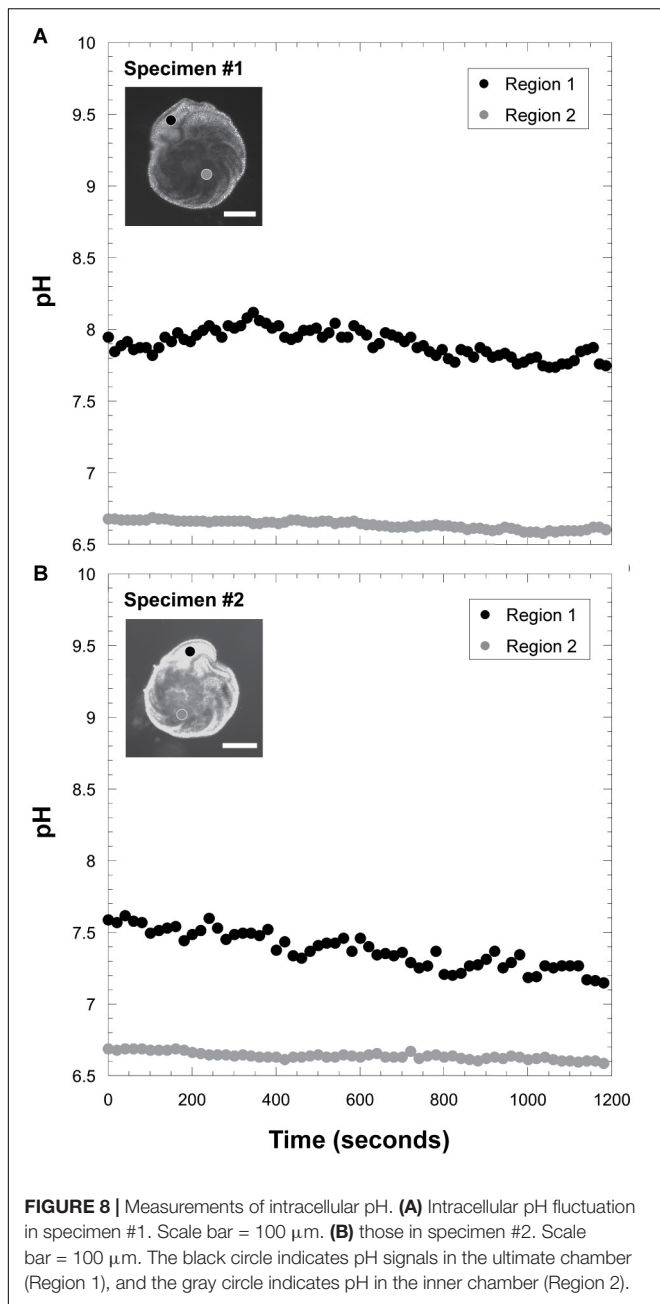
Distribution of Kleptoplasts in *P. opercularis*

The kleptoplasts in *P. opercularis* were distinctively localized along the cell periphery at the dorsum of chambers, beneath the pore plug; these kleptoplasts were flattened (**Figure 1**) (Jauffrais et al., 2018). This arrangement also occurs in haptophytil plastid-bearing *Dinophysis mitra*, in which haptophytil kleptoplasts are localized in the marginal region of the cell (Koike et al., 2005). This pattern of kleptoplastid localization had been found previously in *Elphidium williamsoni* and *E. selseyense*, and *Amphistegina lessonii* demonstrates localization of diatom symbionts at the pore rim (Lee, 2006). However, the close localization between pore-plug and kleptoplast described here has been found only in *P. opercularis* (Jauffrais et al., 2018).

Foraminifera are thought to adjust the size and density of the pores in the test according to the ambient environment, especially in regard to the DO concentration, as the pores function in gas exchange (Moodley and Hess, 1992). In fact, the oxygen microsensor data in our study suggest that the high oxygen production at the dorsal side of *P. opercularis* is associated with its greater abundance of pores compared with that on

the ventral side (**Figure 6**) and responds rapidly to changes in the intensity of light irradiation (**Table 2** and **Figure 7**). In contrast, few or no pores were present on the ventral side; instead, high levels of cellular activities such as pseudopodia extension occurred on the ventral side of *P. opercularis* (**Figure 6**). The oxygen consumption rate was relatively high during constant darkness and at the ventral side; however, bulk specimens were well balanced overall in regard to oxygen production and consumption. These findings support the proposed relationship between the function of the pore and the distribution and configuration of kleptoplasts.

Therefore, we consider that the *P. opercularis* maintains kleptoplasts in the cell periphery just beneath the pore plug to facilitate gas exchange at a position where kleptoplasts can effectively absorb light for photosynthesis. Kleptoplasts may modulate the efficiency of photosynthesis at the cell periphery to produce oxygen and organic materials and thus, may affect the intracellular environment. The intracellular pH in the inner chambers (**Figure 8**) was different between *P. opercularis* and asymbiotic foraminifera, *Cibicides lobatulus* and *Ammonia "beccarii"* (de Nooijer et al., 2008). The former species have higher pH (~ 6.6) (**Figure 8**) whereas the latter asymbiotic species have lower pH (< 6.0). Both species have higher pH at the calcification site, however, the intracellular pH was relatively low in *P. opercularis* ($7.0\sim 8.0$) compared to asymbiotic foraminifera (pH $7.5\sim 8.5$) in the ultimate chamber. Kleptoplasts' effects on intracellular pH environments probably involved calcification of high magnesian calcite of *P. opercularis* (**Figure 8**). The narrow range of pH concentration in this species possibly inhibits elimination of magnesium ion. Chloroplasts require a certain amount of magnesium in general so that it may maintain



intracellular magnesium in a favorable environment for the kleptoplasts. In other words, it may be a strategy to keep the intracellular Mg^{2+} rather than actively increasing Ca^{2+} . Outward proton pumping is known to be associated with foraminiferal calcification, the pH gradient plays an important role for this process (Toyofuku et al., 2017). Thus, the hydrogen ions may not be actively exchanged and the pH gradient between inside and outside the cell does not become dominant. It is possible to explain that the gap between the pH inside and outside the cell is small in our current observation (Figure 8). Therefore, it is assumed that the Mg/Ca in the calcite test of this species is higher (Toyofuku et al., 2000; Toyofuku and Kitazato, 2005)

than other hyaline species compared to results of de Nooijer et al. (2009). However, oxygen production showed little change with increasing levels of light irradiation between 33 and 320 $\mu\text{mol photon m}^{-2} \text{s}^{-1}$ (Table 2 and Figure 7). This finding is similar to the condition in other kleptoplast-bearing and symbiotic algae-bearing foraminifera, in which oxygen production reaches saturation at a light intensity of 30 $\mu\text{mol photon m}^{-2} \text{s}^{-1}$ (Rink et al., 1998; Cesbron et al., 2017). In the case of *P. opercularis*, however, kleptoplast oxygen production presumably is minimal at this light intensity.

The kleptoplasts maintained by *P. opercularis* carry out oxygenic photosynthesis, thereby producing organic materials such as amino acid (Tsuchiya et al., 2018). Consequently, the trophic hierarchy of freshly collected specimens of *P. opercularis* yielded trophic positions of 1.2 and 2.0 (Tsuchiya et al., 2018). The former value indicates the predominant contribution of a primary producer, whereas 100% of the latter value is due to a primary consumer. Therefore, *P. opercularis* has mixotrophic behavior. This was confirmed in our study by the finding that *P. opercularis* retained kleptoplasts longer when food materials were available. It is possible that this mixotrophic behavior allows foraminifera to adapt to conditions of insufficient food, similar to sea slugs (Maeda et al., 2012). *Planoglabratella opercularis* effectively acquires energy through this mixotrophic behavior, they have to frequently retained kleptoplasts.

Interestingly, 11-day cultures of *P. opercularis* indicated the capture of live *Chlorella* cells, according to the presence of diagnostic ultrastructural characteristics of the chloroplast membrane, thylakoids, and starch granules. The cell wall was in a separate vacuole; we could not confirm the presence of other cellular components such as the nucleus, mitochondria, and cellular substrates (Figure 3 and Supplementary Figure S6). The host foraminifera apparently maintained only the chloroplasts of *Chlorella*, rather than entire *Chlorella* cells (Ikeda and Takeda, 1995; Němcová and Kalina, 2000). Note that any enzymatic activity in host vacuoles only affects the cell wall of *Chlorella* (Gerken et al., 2012), leaving its chloroplasts undegraded in the host foraminifera. The electron-dense outer wall was not visible. However, we noted fibrillar structures on the surface of the cell wall, a low-density layer, and an inner membrane (Figure 3A and Supplementary Figure S6F). Moreover, some of the captured *Chlorella* chloroplasts were located beneath the pore plug in the cell periphery (Figure 3B). In a similar phenomenon, endosymbiotic *Chlorella* in *Paramecium bursaria* localize to the host cell periphery; the underlying mechanisms remain unknown (Kodama and Fujishima, 2011). Unlike endosymbionts of *Chlorella* species, localization of kleptoplasts in the cell periphery also occurred in *P. opercularis*. Whether *P. opercularis* maintained the captured *Chlorella* as symbionts or kleptoplasts or digested them as food is unknown. Although we did not determine how long the captured *Chlorella* actually remained in host foraminiferal cells, we did show that *P. opercularis* has the potential to maintain chloroplasts of *Chlorella* temporarily as kleptoplasts after removing the robust cell wall of live *Chlorella* within the host's vacuoles. In fact, the R.I. of autofluorescence recovered on days 6

and 10 in the foraminifera fed live *Chlorella* throughout the culture period (Figure 5A); perhaps the rate of uptake of live *Chlorella* cells was very slow due to the existence of a persistent cell wall.

Acquisition and Maintenance of Kleptoplast

Planoglabratella opercularis acquired kleptoplasts from the diatom cytoplasm, leaving the diatom frustules at the aperture; frustules were not found in the cytoplasm of the host. In fact, the frustules were left behind the host in a trail as *P. opercularis* captured the diatoms (Supplementary Figure S3). This phenomenon was similar to observations in other kleptoplast-bearing foraminifera; for example, *Haynesina germanica* removes diatom frustules by cracking or destroying them at the aperture (Austin et al., 2005). In general, apertural morphology such as tooth-like structures and ventral ornamentations are important for feeding (Austin et al., 2005), selection of food materials (Kitazato, 1992), and chloroplast acquisition (Bernhard and Bowser, 1999). The genus *Elphidium* is thought to capture kleptoplasts in the same manner as does *Haynesina*: the host foraminifera cracks the diatom's frustules and then captures and retains the chloroplast from the diatom cytoplasm (Lopez, 1979).

Foraminifera specifically acquired chloroplasts as kleptoplasts from diatoms rather than from microalgae like *Chlorella*, perhaps because of the diatoms' destructible frustules compared to the relatively indestructible cell walls of the algae. When fed with live *Chlorella* cells, *P. opercularis* acquired *Chlorella* chloroplasts more than 10 days after the mixed culture started. This phenomenon is similar to the kleptoplasty of other foraminiferal species. Even if *P. opercularis* captured *Chlorella* cells, they would be difficult to digest within a short period. For this reason, the kleptoplastid autofluorescence decreased during the experimental period in the cultures fed live *Chlorella* cells. In the case of fed live *Chlorella* throughout the culture period, the autofluorescence was fluctuated on day 10 (Figure 5A). This means that there has an ability to photosynthesize by captured *Chlorella* chloroplasts.

The processes of kleptoplast acquisition and the organisms that are captured differ among host organisms. The dinoflagellate *Dinophysis acuminata* acquires cryptophyte-origin chloroplasts by feeding on ciliate, which has eaten the cryptophyte (Park et al., 2006). The sea slug *E. chlorotica* captures the kleptoplast from the cytoplasm of siphonous green algae by scratching the algal surface with its radular tooth and acquiring chloroplasts in its digestive tract by phagocytosis (Kawaguti and Yamasu, 1965; Rumpho et al., 2000). Foraminifera capture intact cytoplasm of diatoms using their pseudopodia to pull the diatom cytoplasm through the foraminiferal aperture openings; the host cells then digest the cytoplasm of diatoms, leaving behind the chloroplasts as kleptoplasts (Tsuchiya et al., 2015). The processes of kleptoplast acquisition are the same between *V. fragilis* and *P. opercularis*, but they likely differ in the mechanisms by which they maintain kleptoplasts. In the former, kleptoplasts are likely maintained via close proximity to host cytoplasm and

fragmentation of kleptoplastid membranes, while in the latter kleptoplasts exist in the vacuole.

Influence of Food Availability and Lighting Conditions on the Maintenance of Kleptoplasts

The autofluorescence of kleptoplasts in the cytoplasm varied with the duration of food source availability and light irradiation (Figures 5A,B), and reacted rapidly to light irradiation, congruent with observations from Cesbron et al. (2017). The attenuation of kleptoplastid autofluorescence was significantly greater at constant light or 12:12-h light:dark cycle than in constant dark or 24:24-h light:dark cycle. Thus, kleptoplasts were retained in the cytoplasm of *P. opercularis* for 10 days or less when exposed to constant light or a 12:12-h light:dark cycle. The kleptoplasts were degraded by host digestion and probably underwent photoinhibition. Therefore, given the short persistence of the kleptoplasts (<14 days), the host foraminifera must frequently ingest additional diatoms, simultaneously obtaining both kleptoplasts and the food material needed to maintain them. This finding is congruent with *Elphidium williamsoni* that retain functional kleptoplasts at least 15 days (Jauffrais et al., 2019a). Kleptoplastid autofluorescence of the host foraminifera increased on day 2 in the fed experimental group of heat-killed *Chlorella*. This phenomenon may be caused by the host foraminiferal activity. The degradation of the kleptoplastid thylakoid membranes on day 11 of culture was greater in the unfed cultures than in the fed experimental groups. This phenomenon may affect the activity of the host foraminifera, and as a result, it is considered that the activity of kleptoplasts also increased. It is possible that some unknown mechanism are existed to avoid digestion of kleptoplasts in the fed experimental group.

Planoglabratella opercularis retains kleptoplasts for less time than does *E. excavatum* (Correia and Lee, 2002b). However, the light irradiance level was approximately five times higher in our culture experiment than in the experiment that yielded the previous observation (60 μ E) (Correia and Lee, 2002b). Although we cannot directly compare the kleptoplast retention times between these two hosts, kleptoplasts were retained for at least 8 weeks in *E. excavatum*, distinctively longer than in *P. opercularis* (Correia and Lee, 2002b). Even though kleptoplast retention times differ between host species, within a species, retention time is longer in the dark than in the light (Lopez, 1979; Correia and Lee, 2002b; Grzymiski et al., 2002; Jauffrais et al., 2016). Kleptoplasts were retained for as long as 1 year in the dark in *Nonionella stella* collected under the euphotic zone at a depth of ~600 m in the Santa Barbara basin (Grzymiski et al., 2002). The prolonged retention time of kleptoplasts in *P. opercularis* exposed to constant dark supports this observation. Interestingly, *P. opercularis* still retains some autofluorescence (37%) on day 14 of culture in a 24:24-h light:dark cycle, suggesting that although prolonged exposure to light tended to damage kleptoplasts, prolonged exposure to dark may have had a restorative effect. In general, prolonged exposure to high-intensity light may lead to photoinhibition of kleptoplasts through the generation of

reactive oxygen species. In fact, peroxisomes and mitochondria were frequently present around kleptoplasts (Figures 1A,B). This phenomenon is thought to be a protective mechanism by which the host foraminifera can degrade excess reactive oxygen produced in the kleptoplasts.

CONCLUSION

We determined the process of the acquisition and maintenance of kleptoplasts in *P. opercularis* and has a key factor for foraminiferal ecology in the metabolic and adaptive mechanisms of this species. *Planoglabratella opercularis* retained kleptoplasts, most of which likely originated from Bacillariophyceae diatom species in light of their high homology to these periphytic diatoms, utilize wide range of diatom species from low salinity waters to marine environments.

The autofluorescence of kleptoplasts in the host *P. opercularis* cytoplasm varied with sources, availability and available period of foods and with light conditions that is correspond well to the trophic requirements, they behave as primary producer in the high-light irradiance, whereas behave as primary producer in low-light irradiance. In other words, *P. opercularis* do not mainly utilize photosynthates but maintain their nutrient sources through predation alone when food is available. This suggests that *P. opercularis* behaves as a mixotroph, and consistent with the estimated trophic position (Tsuchiya et al., 2018). We presume that the short-lived photosynthesis of kleptoplast is due to the lack of a nuclear gene to control it. Thus, we speculate that the kleptoplasts itself show only a short period of retention time, and the photosynthetic activity cannot be maintained. Host foraminifera acquire diatom cells frequently, simultaneously obtaining kleptoplasts and the food material to maintain them within < 14 days. Kleptoplasts transmitted vertically to asexually reproducing juveniles that they have potentially to take photosynthates for up to 5 days without introduction of kleptoplasts.

It also has effectiveness of kleptoplast retention for controlling pH condition in vesicles. Ocean acidification is in progress and affect the calcifier of foraminifera. Effect of ocean acidification controls not only density of foraminiferal test, but also test ornamentation. When apertural ornamentation weakened, foraminifera cannot capture kleptoplast from diatom cell. The effect of kleptoplast-induced changes in intracellular pH must also be taken into account to evaluate the effect of ocean acidification on foraminifera.

Host species of *P. opercularis* can survive in low-temperature (10°C) and low-salinity (25) environments revealed by culture experiment (Tsuchiya et al., 2014). Thus, the effect of environmental changes, especially in low temperature and low salinity environments, to *P. opercularis* may be limited, because, a diverse kleptoplasts from low-salinity to marine environments was retained into cell cytoplasm. It is possible that the persistence of local populations of *P. opercularis* is thus influenced by endobiont ecology, role of retained kleptoplasts and host food resource usage.

DATA AVAILABILITY STATEMENT

The datasets presented in this study can be found in online repositories. The names of the repository/repositories and accession number(s) can be found in the article/Supplementary Material.

AUTHOR CONTRIBUTIONS

MT conceived and designed the experiments. MT, SM, and KO performed the experiments for culture and microsensor observation and analyzed the data. MT, SM, AT, and KU performed the experiments for TEM observation. MT, SM, KT, and YS performed the experiments for molecular work. TT performed the experiments for intracellular pH measurements. MT, KO, AT, and KU contributed reagents, materials, and analysis tools. MT drafted the manuscript. All authors contributed to improve the manuscript and approved the submission.

FUNDING

This work was supported by a Grants-in-Aid for Scientific Research (Nos. 24340131 and 17K05696 to MT) of Japan Society for the Promotion of Science (JSPS). The funders had no role in study design, data collection and analysis, decision to publish, or preparation of the manuscript.

ACKNOWLEDGMENTS

We are grateful to Dr. Angel Borja, Guest Associate Editor of Frontiers in Marine Science, the two reviewers for their valuable comments on this manuscript, Mr. Shigeru Shimamura and Mr. Masaru Kawato (JAMSTEC) for their technical assistance in the genetic work, Dr. Yukiko Nagai and Ms. Sachiko Kawada (JAMSTEC) for their technical support in the pH observation, and Dr. Taro Maeda (National Institutes of Natural Sciences) for his helpful comments on the experimental design.

SUPPLEMENTARY MATERIAL

The Supplementary Material for this article can be found online at: <https://www.frontiersin.org/articles/10.3389/fmars.2020.00585/full#supplementary-material>

FIGURE S1 | Illustration of experimental design for respiration rate and oxygen production measurements. (A) Overall setting for culture experiment. (B) The microsensor measurements was conducted in a small capillary tube, (C) and in a MicroRespiration Chamber.

FIGURE S2 | Autofluorescence and colors of cytoplasm in reproduced juvenile specimens. (A,B) Color of cytoplasm and autofluorescence of three-chambered juveniles. No autofluorescence signals in the third chamber. Scale bar = 500 μm. (C,D) Color of cytoplasm and autofluorescence visible two days after reproduction in the four-chambered juvenile. Scale bar = 50 μm. (E,F) Cytoplasm lacking color and weak autofluorescence after 5 days. Scale bar = 50 μm. (G,H) Diatom cells,

cytoplasm color, and autofluorescence were recovered in five-chambered juveniles after the addition of diatom cells for food. **(I,J)** Two days after addition of diatom cells, cytoplasm color and autofluorescence were completely recovered in all chambers. Scale bar = 500 μm .

FIGURE S3 | Capture of diatom within the *Planoglabratella opercularis* pseudopodial network. Live diatom cells were drawn toward the foraminiferal cell (arrowheads), leaving diatom frustules behind (arrow). Scale bar = 100 μm .

FIGURE S4 | Transmission electron micrographs (TEMs) of unfed cultures of *Planoglabratella opercularis*. TEMs indicate ultrastructural changes among *P. opercularis* cultured for **(A,B)** 0, **(C,D)** 2, or **(E,F)** 11 days without food. Kleptoplast (*), food vacuoles (fv), lipid (l), mitochondria (m), and nucleus (n). Scale bar = 2 μm **(A,C,F)**; 500 nm **(B)**; 1 μm **(D)**; 5 μm **(E)**.

FIGURE S5 | Transmission electron micrographs (TEMs) of *Planoglabratella opercularis* cultures fed with heat-killed *Chlorella*. TEMs indicate ultrastructural changes between *P. opercularis* fed heat-killed *Chlorella* cultured for **(A,B)** 2 or **(C-F)** 11 days. Intact kleptoplast (*), scale bar = 2 μm **(A)**, 1 μm **(B)**. **(C)** Degraded kleptoplast (k). Scale bar = 2 μm . **(D)** Numerous heat-killed *Chlorella* in food vacuoles (fv), lipid (l). Scale bar = 2 μm . **(E)** Magnified degraded kleptoplast in **(C)**. Thylakoids are clearly visible but outer membranes are degraded. Scale bar = 1 μm . **(F)** Thylakoid membranes and stroma are discretely situated. Scale bar = 1 μm .

FIGURE S6 | Transmission electron micrographs (TEMs) of *Planoglabratella opercularis* cultures fed live *Chlorella*. TEMs indicate the ultrastructural differences among *P. opercularis* fed live *Chlorella* cultured for **(A,B)** 2 or **(C-F)** 11 days. Nucleus (n), kleptoplast (*), lipid (l), mitochondria (m), food vacuole (fv). *Chlorella* (ch), cell wall of captured *Chlorella* (arrowheads). **(A)** Scale bar = 5 μm .

(B) Scale bar = 2 μm . **(C)** Scale bar = 5 μm . **(D)** Scale bar = 2 μm . **(E)** Intact *Chlorella* chloroplast and the residues of food materials in the food vacuole (fv). Scale bar = 1 μm . **(F)** Fractionated cell wall of *Chlorella* (arrowheads). Fibrillar structures on the surface of the *Chlorella* cell wall, low-density layer, and inner membrane are visible. Dense mitochondria (m), peroxisomes (p) are present. Scale bar = 1 μm .

FIGURE S7 | Phylogenetic tree of the internal transcribed spacers (ITS) of nuclear rRNA for host *Planoglabratella* species based on Bayesian inference. Numbers above the internal branches at the nodes indicate the posterior probabilities. Accession numbers follow the species names.

FIGURE S8 | Statistical analyses of the autofluorescence during the culture periods. Data represent mean \pm standard deviation during the culture periods in each culture condition for **(A)** food conditions and for **(B)** light conditions (Two-way ANOVA $P < 0.05$). An asterisk denotes significant differences between each condition.

FIGURE S9 | Statistical analyses of the autofluorescence fluctuation during the culture period for **(A)** food conditions and for **(B)** light conditions. Data represent mean \pm standard deviation during the culture periods in each culture condition for **(A)** food conditions and for **(B)** light conditions. Different letters stand for significant difference (t -test, $p < 0.05$).

FIGURE S10 | Statistical analyses of the pH fluctuation during the culture period. Data represent mean \pm standard deviation during the culture periods for **(A)** specimen #1 and for **(B)** specimen #2 (t -test, $P < 0.05$). The black box indicates pH values in the ultimate chamber (Region 1), and the gray box indicates pH in the inner chamber (Region 2). An asterisk denotes significant differences between each site.

REFERENCES

- Austin, H. J., Austin, W. E. N., and Paterson, D. M. (2005). Extracellular cracking and content remove of the benthic diatom *Pleurosigma angulatum* (Quekett) by the benthic foraminifera *Haynesina germanica* (Ehrenberg). *Mar. Micropaleontol.* 57, 68–73. doi: 10.1016/j.marmicro.2005.07.002
- Bé, A. W. H., Spero, H. J., and Anderson, O. R. (1982). Effects of symbiont elimination and reinfection on the life processes of the planktonic foraminifer *Globigerinoides sacculifer*. *Mar. Biol.* 70, 73–86. doi: 10.1007/BF00397298
- Bedoshvili, Y. D., Popkova, T. P., and Likhoshway, V. (2009). Chloroplast structure of diatoms of different classes. *Cell. Tissue. Biol.* 51, 346–351. doi: 10.1134/S1990519X09030122
- Bernhard, J. M. (2003). Potential symbionts in bathyal foraminifera. *Science* 299:861. doi: 10.1126/science.1077314
- Bernhard, J. M., and Bowser, S. S. (1999). Benthic foraminifera of dysoxic sediments: chloroplast sequestration and functional morphology. *Earth Sci. Rev.* 46, 149–165. doi: 10.1016/S0012-8252(99)00017-3
- Cesbron, F., Geslin, E., Le Kieffre, C., Jauffrais, T., Nardelli, M. P., Langlet, D., et al. (2017). Sequestered chloroplasts in the benthic foraminifer *Haynesina germanica*: cellular organization, oxygen fluxes and potential ecological implications. *J. Foramin. Res.* 47, 268–278. doi: 10.2113/gsjfr.47.3.268
- Chai, J., and Lee, J. J. (2000). Recognition, establishment and maintenance of diatom endosymbiosis in foraminifera. *Micropaleontology* 46(suppl. 1), 182–195.
- Chronopoulou, P.-M., Salonen, I., Bird, C., Reichart, G.-J., and Koho, K. A. (2019). Metabarcoding insights into the trophic behavior and identity of intertidal benthic foraminifera. *Front. Microbiol.* 10:1169. doi: 10.3389/fmicb.2019.01169
- Correia, M. J., and Lee, J. J. (2000). Chloroplast retention by *Elphidium excavatum* (Terquem). Is it a selective process? *Symbiosis* 29, 323–355.
- Correia, M. J., and Lee, J. J. (2002a). Fine structure of the plastids retained by the foraminifer *Elphidium excavatum* (Terquem). *Symbiosis* 32, 15–26.
- Correia, M. J., and Lee, J. J. (2002b). How long do the plastids retained by *Elphidium excavatum* (Terquem) last in their host? *Symbiosis* 32, 27–38.
- de Nooijer, L. J., Toyofuku, T., and Kitazato, H. (2009). Foraminifera promote calcification by elevating their intracellular pH. *Proc. Natl. Acad. Sci. U.S.A.* 106, 15374–15378. doi: 10.1073/pnas.0904306106
- de Nooijer, L. J., Toyofuku, T., Oguri, K., Nomaki, H., and Kitazato, H. (2008). Intracellular pH distribution in foraminifera determined by the fluorescent probe HPTS. *Limnol. Oceanogr. Meth.* 6, 610–618. doi: 10.4319/lom.2008.6.610
- d'Orbigny, A. D. (1839). *Foraminifères, in de la Sagra R., Histoire Physique, Politique et Naturelle de l'île de Cuba*. Paris: A. Bertrand, 1–224.
- Felsenstein, J. (1981). Evolutionary trees from DNA sequences: a maximum likelihood approach. *J. Mol. Evol.* 17, 368–376. doi: 10.1007/BF01734359
- Gerken, H. G., Donohoe, B., and Knoshaug, E. P. (2012). Enzymatic cell wall degradation of *Chlorella vulgaris* and other microalgae for biofuels production. *Planta* 237, 239–253. doi: 10.1007/s00425-012-1765-0
- Grzyski, J., Schofield, O. M., Falkowski, P. G., and Bernhard, J. M. (2002). The function of plastid in the deep-sea benthic foraminifer *Nonionella stella*. *Limnol. Oceanogr.* 47, 1569–1580. doi: 10.4319/lo.2002.47.6.1569
- Guillou, L., Chrétiennot-Dinet, M.-J., Medlin, L. K., Claustre, H., Loiseaux-de Goër, S., and Vault, D. (1999). *Bolidomonas*: a new genus with two species belonging to a new algal class, the Bolidophyceae (Heterokonta). *J. Phycol.* 35, 368–381. doi: 10.1046/j.1529-8817.1999.3520368.x
- Guindon, S., Dufayard, J. F., Lefort, V., Anisimova, M., Hordijk, W., and Gascuel, O. (2010). New algorithms and methods to estimate maximum-likelihood phylogenies: assessing the performance of PhyML 3.0. *Syst. Biol.* 5, 307–321. doi: 10.1093/sysbio/syq010
- Hallock, P. (1981). Algal symbiosis: a mathematical analysis. *Mar. Biol.* 62, 249–255. doi: 10.1007/BF00397691
- Hallock, P. (1999). "Symbiont-bearing foraminifera," in *Modern Foraminifera*, ed. B. K. Sen Gupta (Dordrecht: Kluwer Academic Publishers), 123–139. doi: 10.1007/0-306-48104-9_8
- Heinz, P., Kitazato, H., Schmiel, G., and Hemleben, C. (2001). Response of deep-sea benthic foraminifera from the Mediterranean Sea to simulated phytoplankton pulses under laboratory conditions. *J. Foramin. Res.* 31, 210–227. doi: 10.2113/31.3.210
- Hemleben, C., Spindler, M., and Anderson, O. R. (1989). *Modern Planktonic Foraminifera*. New York, NY: Springer Verlag.
- Huber, T., Faulkner, G., and Hugenholtz, P. (2004). Bellerophon: a program to detect chimeric sequences in multiple sequence alignments. *Bioinformatics* 20, 2317–2319. doi: 10.1093/bioinformatics/bth226

- Huelsensbeck, J. P., and Ronquist, F. (2001). MRBAYES: Bayesian inference of phylogenetic trees. *Bioinformatics* 17, 754–755. doi: 10.1093/bioinformatics/17.8.754
- Ikeda, T., and Takeda, H. (1995). Species-specific differences of pyrenoids in *Chlorella* (Chlorophyta). *J. Phycol.* 31, 813–818. doi: 10.1111/j.0022-3646.1995.00813.x
- Jauffrais, T., Jesus, B., Metzger, E., Mouget, J. L., Jorissen, F., and Geslin, E. (2016). Effect of light on photosynthetic efficiency of sequestered chloroplasts in intertidal benthic foraminifera (*Haynesina germanica* and *Ammonia tepida*). *Biogeosciences* 13, 2715–2726. doi: 10.5194/bg-13-2715-2016
- Jauffrais, T., LeKieffre, C., Koho, K. A., Tsuchiya, M., Schweizer, M., Bernhard, J. M., et al. (2018). Ultrastructure and distribution of sequestered chloroplasts in benthic foraminifera from shallow-water (photic) habitats. *Mar. Micropaleontol.* 138, 46–62. doi: 10.1016/j.marmicro.2017.10.003
- Jauffrais, T., LeKieffre, C., Schweizer, M., Geslin, E., Metzger, E., Bernhard, J. M., et al. (2019a). Kleptoplastidic benthic foraminifera from aphotic habitats: insights into assimilation of inorganic C, N and S studied with sub-cellular resolution. *Environ. Microbiol.* 21, 125–141. doi: 10.1111/1462-2920.14433
- Jauffrais, T., LeKieffre, C., Schweizer, M., Jesus, B., Metzger, E., and Geslin, E. (2019b). Response of a kleptoplastidic foraminifer to heterotrophic starvation: photosynthesis and lipid droplet biogenesis. *FEMS Microbiol. Ecol.* 95:fiz046. doi: 10.1093/femsec/fiz046
- Kawaguti, S., and Yamasu, T. (1965). Electron microscopy on the symbiosis between an elysiid gastropod and chloroplasts of a green alga. *Biol. J. Okayama Univ.* 11, 57–65.
- Kitazato, H. (1984). “Microhabitats of benthic foraminifera and their application to fossil assemblages,” in *Benthos '83; 2nd International Symposium on Benthic Foraminifera*, ed. H. J. Oertli (Courbevoie: Elf-Aquitaine), 339–344.
- Kitazato, H. (1992). “Pseudopodia of benthic foraminifera and their relationship to the test morphology,” in *Studies in Benthic Foraminifera, BENTHOS '90* (Tokyo: Tokai University Press), 103–108.
- Kitazato, H. (1994). Foraminiferal microhabitats in four marine environments around Japan. *Mar. Micropaleontol.* 24, 29–41. doi: 10.1016/0377-8398(94)90009-4
- Kodama, Y., and Fujishima, M. (2011). Endosymbiosis of *Chlorella* species to the ciliate *Paramecium bursaria* alters the distribution of the host's trichocysts beneath the host cell cortex. *Protoplasma* 248, 325–337. doi: 10.1007/s00709-010-0175-z
- Koike, K., Sekiguchi, H., Kobiyama, A., Takishita, K., Kawachi, M., Koike, K., et al. (2005). A novel type of kleptoplastid in *Dinophysis* (Dinophyceae): presence of haptophyte-type plastid in *Dinophysis mitra*. *Protist* 156, 225–237. doi: 10.1016/j.protis.2005.04.002
- Lee, J. J. (2006). Algal symbiosis in larger foraminifera. *Symbiosis* 42, 63–75.
- Lee, J. J., Cervasco, M. H., Morales, J., Billik, M., Fine, M., and Levy, O. (2010). Symbiosis drove cellular evolution. *Symbiosis* 51, 13–25. doi: 10.1007/s13199-010-0056-4
- Lee, J. J., Sang, K., ter Kuile, B., Strauss, E., Lee, P. J., and Faber, W. W. Jr. (1991). Nutritional and related experiments on laboratory maintenance of three species of symbiont-bearing, large foraminifera. *Mar. Biol.* 109, 417–425. doi: 10.1007/BF01313507
- LeKieffre, C., Jauffrais, T., Geslin, E., Jesus, B., Bernhard, J. M., Giovanni, M.-E., et al. (2018). Inorganic carbon and nitrogen assimilation in cellular compartments of a benthic kleptoplastidic foraminifer. *Sci. Rep.* 8:10140. doi: 10.1038/s41598-018-28455-1
- Lopez, E. (1979). Algal chloroplasts in the protoplasm of three species of benthic foraminifera: taxonomic affinity, viability and persistence. *Mar. Biol.* 53, 201–211. doi: 10.1007/BF00952427
- Maeda, T., Hirose, E., Chikaraishi, Y., Kawato, M., Takishita, K., Yoshida, T., et al. (2012). Algivore or Phototroph? *Plakobranchnus ocellatus* (Gastropoda) continuously acquires kleptoplasts and nutrition from multiple algal species in nature. *PLoS One* 7:e42024. doi: 10.1371/journal.pone.0042024
- Moodley, L., and Hess, C. (1992). Tolerance of infaunal benthic foraminifera for low and high oxygen concentrations. *Biol. Bull.* 183, 94–98. doi: 10.2307/1542410
- Němcová, Y., and Kalina, T. (2000). Cell wall development, microfibril and pyrenoid structure in type strain of *Chlorella vulgaris*, *C. kessleri*, *C. sorokiniana* compared with *C. luteoviridis* (Trebouxiophyceae, Chlorophyta). *Arch. Hydrobiol. Suppl. Algol. Stud.* 100, 95–105.
- Nylander, J. A. A. (2004). *MrModeltest v2. Program Distributed by the Author*. Uppsala: Uppsala University.
- Park, M. G., Kim, S., Kim, H. S., Myung, G., Kang, Y. G., and Yih, W. (2006). First successful culture of the marine dinoflagellate *Dinophysis acuminata*. *Aquat. Microb. Ecol.* 45, 101–106. doi: 10.3354/ame045101
- Pawlowski, J. (2000). Introduction to the molecular systematics of foraminifera. *Micropaleontology* 46(suppl. 1), 1–12. doi: 10.1002/9781444313949.ch1
- Pillet, L., de Vargas, C., and Pawlowski, J. (2011). Molecular identification of sequestered diatom chloroplasts and kleptoplastid in foraminifera. *Protist* 162, 394–404. doi: 10.1016/j.protis.2010.10.001
- Rambaut, A. (1996). *Se-Al ver. 2.0a11: Sequence Alignment Editor*. Available online at: <http://evolve.zoo.ox.ac.uk/software/seal/> (accessed July 7, 2020).
- Rink, S., Kühl, M., Bijma, J., and Spero, H. J. (1998). Microsensor studies of photosynthesis and respiration in the symbiotic foraminifer *Orbulina universa*. *Mar. Biol.* 131, 583–595. doi: 10.1007/s002270050350
- Rodriguez, F., Oliver, J. L., Marin, A., and Medina, J. R. (1990). The general stochastic model of nucleotide substitutions. *J. Theor. Biol.* 142, 485–501. doi: 10.1016/S0022-5193(05)80104-3
- Röttger, R. (1974). Larger foraminifera: reproduction and early stages of development in *Heterostegina depressa*. *Mar. Biol.* 26, 5–12. doi: 10.1007/BF00389081
- Rumpho, M. E., Summer, E. J., and Manhart, J. R. (2000). Solar-powered sea slugs. Mullusc/algal chloroplast symbiosis. *Plant. Physiol.* 123, 29–38. doi: 10.1104/pp.123.1.29
- Sawai, Y. (2001). Distribution of living and dead diatoms in tidal wetlands of northern Japan: relations to taphonomy. *Palaeogeogr. Palaeoclimatol. Palaeoecol.* 173, 125–141. doi: 10.1016/S0031-0182(01)00313-3
- Schneider, C. A., Rasband, W. S., and Eliceiri, K. W. (2012). NIH Image to ImageJ: 25 years of image analysis. *Nature methods* 9, 671–675. doi: 10.1038/nmeth.2089
- Takishita, K., Nakano, K., and Uchida, A. (1999). Preliminary phylogenetic analysis of plastid-encoded genes from an anomalously pigmented dinoflagellate *Gymnodinium mikimotoi* (Gymnodiniales, Dinophyta). *Phycol. Res.* 47, 257–262. doi: 10.1046/j.1440-1835.1999.00175.x
- Thompson, J. D., Higgins, D. G., and Gibson, T. J. (1994). CLUSTAL W: improving the sensitivity of progressive multiple sequence alignment through sequence weighting, position specific gap penalties and weight matrix choice. *Nucleic Acids Res.* 22, 4673–4680. doi: 10.1093/nar/22.22.4673
- Toyofuku, T., de Nooijer, L. J., Yamamoto, H., and Kitazato, H. (2008). Real-time visualization of calcium ion activity in shallow benthic foraminiferal cells using the fluorescent indicator Fluo-3 AM. *Geochem. Geophys. Geosyst.* 9:Q05005. doi: 10.1029/2007GC001772
- Toyofuku, T., and Kitazato, H. (2005). Micromapping of Mg/Ca values in cultured specimens of the high-magnesium benthic foraminifera. *Geochem. Geophys. Geosyst.* 6:Q11P05. doi: 10.1029/2005GC000961
- Toyofuku, T., Kitazato, H., Kawahata, H., Tsuchiya, M., and Nohara, M. (2000). Evaluation of Mg/Ca thermometry in foraminifera: comparison of experimental results and measurements in nature. *Paleoceanography* 15, 456–464. doi: 10.1029/1999pa000460
- Toyofuku, T., Matsuo, M. Y., de Nooijer, L. J., Nagai, Y., Kawada, S., Fujita, K., et al. (2017). Proton pumping accompanies calcification in foraminifera. *Nat. Commun.* 8:14145. doi: 10.1038/ncomms14145
- Tsuchiya, M., Aizawa, M., Suzuki-Kanesaki, H., and Kitazato, H. (1994). Life history of *Glauertella opercularis* (d'Orbigny): observations and experiments. *PaleoBios* 16:62.
- Tsuchiya, M., Chikaraishi, Y., Nomaki, H., Sasaki, Y., Tame, A., Uematsu, K., et al. (2018). Compound-specific isotope analysis of benthic foraminifer amino acids suggests microhabitat variability in rocky-shore environments. *Ecol. Evol.* 8, 8380–8395. doi: 10.1002/ece3.4358
- Tsuchiya, M., Grimm, G. W., Heinz, P., Stögerer, K., Ertan, K. T., Collen, J., et al. (2009). Ribosomal DNA shows extremely low genetic divergence in a world-wide distributed, but disjunct and highly adapted marine protozoan (*Virgulina fragilis*, Foraminiferida). *Mar. Micropaleontol.* 70, 8–19. doi: 10.1016/j.marmicro.2008.10.001
- Tsuchiya, M., Kitazato, H., and Pawlowski, J. (2000). Phylogenetic relationship among species of Glauertellidae (Foraminifera) inferred from ribosomal

- DNA sequences: comparison with morphological and reproductive data. *Micropaleontology* 46(suppl. 1), 13–20.
- Tsuchiya, M., Kitazato, H., and Pawlowski, J. (2003). Analysis of internal transcribed spacer of ribosomal DNA reveals cryptic speciation in *Planoglabratella opercularis*. *J. Foramin. Res.* 33, 285–293. doi: 10.2113/0330285
- Tsuchiya, M., Takahara, K., Aizawa, M., Suzuki-Kanesaki, H., Toyofuku, T., and Kitazato, H. (2014). “How has foraminiferal genetic diversity developed? A case study of *Planoglabratella opercularis* and the species concept inferred from its ecology, distribution, genetics, and breeding behavior,” in *Experimental Approaches in Foraminifera: Collection, Maintenance and Experiments: Environmental Science Series*, eds H. Kitazato and J. Bernhard (Tokyo: Springer), 133–162. doi: 10.1007/978-4-431-54388-6_9
- Tsuchiya, M., Toyofuku, T., Uematsu, K., Brüchert, V., Collen, J., Yamamoto, H., et al. (2015). Cytologic and genetic characteristics of endobiotic bacteria and kleptoplasts of *Virgulinema fragilis* (Foraminifera). *J. Eukaryot. Microbiol.* 62, 454–469. doi: 10.1111/jeu.12200
- Van Steenkiste, N. W. L., Stephenson, I., Herranz, M., Husnik, F., Keeling, P. J., and Leander, B. S. (2019). A new case of kleptoplasty in animals: marine flatworms steal functional plastids from diatoms. *Sci. Adv.* 5:eaaw4337. doi: 10.1126/sciadv.aaw4337
- Waugh, G. R., and Clark, K. B. (1986). Seasonal and geographic variation in chlorophyll level of *Elysia tuca* (Ascoglossa, Opisthobranchia). *Mar. Biol.* 92, 483–487. doi: 10.1007/BF00392508
- Conflict of Interest:** AT and KU are employed by the company Marine Works Japan, Ltd.
- The remaining authors declare that the research was conducted in the absence of any commercial or financial relationships that could be construed as a potential conflict of interest.
- Copyright © 2020 Tsuchiya, Miyawaki, Oguri, Toyofuku, Tame, Uematsu, Takeda, Sakai, Miyake and Maruyama. This is an open-access article distributed under the terms of the Creative Commons Attribution License (CC BY). The use, distribution or reproduction in other forums is permitted, provided the original author(s) and the copyright owner(s) are credited and that the original publication in this journal is cited, in accordance with accepted academic practice. No use, distribution or reproduction is permitted which does not comply with these terms.